Scirrhous gastric carcinoma diffusely infiltrates a broad region of the stomach and is frequently associated with metastasis to lymph nodes and peritoneal dissemination and therefore has the worst prognosis among the various types of gastric cancer (35). Blocking of the survival signaling mediated by Ossa, which sensitizes the cancer cells to stress-induced apoptosis, may be a novel therapeutic approach for gastric scirrhous carcinoma cells.

MATERIALS AND METHODS

Plasmids, antibodies, and reagents. Full-length cDNAs of human Ossa/C9orf10 and IGF-II mRNA-binding protein 1 (IMP-1) from 44As3 cells were amplified by reverse transcription (RT)-PCR. Mutant forms of C9orf10 lacking the cytoplasmic tail (N1, amino acids [aa] 1 to 339; N2, aa 1 to 405; N3, aa 1 to 570) were generated by PCR-based techniques. To make Flag-tagged C9orf10, a DNA fragment encoding the Flag tag was inserted 3′ to C9orf10. GST-C9orf10 fragments were generated by cloning of PCR-amplified cDNA of C9orf10 into pGEX4T2 (Amersham Pharmacia). The plasmids encoding the IGF-II leader 3 mRNA were donated by J. Christiansen (University of Copenhagen). Full-length cDNA of IMP-1 was amplified by RT-PCR, and the region encoding KH domains 1 to 4 was subcloned into pGEX4T2. To generate the recombinant retrovirus, cDNAs were subcloned into a pDON-AI vector (Takara). A monoclonal antibody that recognizes the Flag tag was purchased from Sigma. A goat polyclonal antibody that recognizes IMP-1 was purchased from Santa Cruz Biotechnology, Inc. To generate polyclonal antibodies against C9orf10, anti-C9orf10-N and -C9orf10-C antibodies were obtained by rabbit immunization with C9orf10 aa 1 to 80 or 829 to 1119 fused to glutathione *S*-transferase (GST). Monoclonal antibodies for phosphotyrosine (4G10) and Ki-67 were obtained from Upstate and DakoCytomation, respectively. Antibodies to c-Src (clone GD11), Fyn, and c-Yes were purchased from Upstate Biotechnology, Santa Cruz, and Transduction Laboratories, respectively. Antibodies to phospho-Src family Tyr416 or Tyr527 (corresponding to Tyr419 and Tyr530 of human Src, respectively), anti-phospho-p53 (Ser15), and anti-phospho-ATM (Ser1981) were from Cell Signaling. Anti-phospho-Src Tyr416 cross-reacts with c-Src, Fyn, c-Yes, Lyn, Lck, and Hck, and anti-phospho-Src Tyr527 cross-reacts with c-Src, Fyn, c-Yes, Fgr, and Yrk. Rabbit polyclonal antibodies for pan-Src (Src2), which reacts with Src, Fyn, Ye,s and Fgr, and anti-PI3-kinase p85α were from Santa Cruz. The SFK inhibitor 4-amino-5-(4-chlorophenyl)-7-(*t*-butyl)pyrazolo[3,4-d]pyrimidine (PP2) and the structural analog 4-amino-7-phenylpyrazolo[3,4-d]pyrimidine (PP3) were purchased from Calbiochem. The DeadEnd colorimetric terminal deoxynucleotidyl-transferase-mediated dUTP-biotin nick end labeling (TUNEL) system was purchased from Promega.

Cell culture, transfection, and retrovirus infection. The 44As3 and NKPS gastric cancer cell lines were cultured in RPMI 1640 medium supplemented with 10% fetal bovine serum. The SYF cell line was purchased from the American Type Culture Collection. Cos1 cells were cultured in Dulbecco modified Eagle medium with 10% fetal bovine serum. For transient expression assays, Cos1 cells and gastric cancer cells were transfected with plasmid DNA by using Lipofectamine 2000 reagent (Invitrogen). Recombinant retroviral plasmid pDON-AI was cotransfected with the pCL-10A1 retrovirus packaging vector (IMGENEX) into 293gp cells to allow the production of retroviral particles. Gastric cancer cells were infected with retroviruses for the transient expression of mutant C9orf10 proteins and used for experiments 48 h after infection. For some experiments, 44As3 or NKPS cells stably overexpressing wild-type C9orf10 were established after retrovirus infection through selection in medium containing G418 (600 μg/ml). In some experiments, cells were irradiated with UV-C by using UV-linker (FS-800; Funakoshi).

Construction of stealth siRNA and miR RNA interference (RNAi) vectors. Stealth small interfering RNA (siRNA) of C9orf10 was synthesized as follows (Invitrogen): Sense-1, 5′-CAAACCAUAUCAGCGGGAACAAGAU-3′; Antisense-1, 5′-AUCUUGUUCCCGCUGAUAUGGUUUG-3′; Sense-2, 5′-CAAACAAAGGCAGAAGGCUCGUCCA-3′; Antisense-2, 5′-UGGACGAGCCUUCUGCCUUUGUUUG-3′. The control siRNA (scramble II duplex, 5′-GCGCGCUUUGUAGGAUUCGdTdT-3′) was purchased from Dharmacon. siRNAs were incorporated into cells with Lipofectamine 2000 according to the manufacturer's instructions (Invitrogen). Assays were performed at 72 h posttreatment.

A system stably expressing siRNA was generated with the BLOCK-IT Pol II miR RNAi expression vector kit (Invitrogen) according to the manufacturer's instructions. In the generation of the miR RNAi vector for humans, C9orf10 was chosen as the target sequence with the forward primer 5′-TGCTGTGTTCCCGCTGATATGGTTTGGTTTTGGCCACTGACTGACCAAACCATCAGCGGGAACA-3′ and the reverse primer 5′-CCTGTGTTCCCGCTGATGGTTTGGTCAGTCAGTGGCCAAAACCAAACCATATCAGCGGGAACAC-3′. Cells stably expressing the microRNA vector for C9orf10 and LacZ were established and cultured in medium containing blasticidin (Invitrogen) at a concentration of 10 μg/ml for 3 weeks.

Immunoprecipitation and immunoblotting. Cell lysates were prepared with protease inhibitors in PLC buffer (50 mM HEPES [pH 7.5], 150 mM NaCl, 1.5 mM $MgCl_2$, 1 mM EGTA, 10% glycerol, 100 mM NaF, 1 mM Na_3VO_4, 1% Triton X-100). To precipitate the proteins, 1 μg of monoclonal antibody or affinity-purified polyclonal antibody was incubated with 500 μg of cell lysate for 2 h at 4°C and then precipitated with protein G-agarose for 1 h at 4°C. Immunoprecipitates were extensively washed with PLC buffer, separated by sodium dodecyl sulfate-polyacrylamide gel electrophoresis (SDS-PAGE), and immunoblotted.

RT-PCR. The presence of IGF-II mRNA bound to the C9orf10 complex was verified by RT-PCR analysis. Following immunoprecipitation of Flag-tagged C9orf10 with anti-Flag M2 agarose in the presence of RNase inhibitor (100 U/ml; Toyobo), RNA was extracted from the agarose beads with 1 ml of Isogen (Nippon Gene) according to the manufacturer's instructions. The isolated RNA was reverse transcribed with random primers for cDNA synthesis. The cDNA was used for PCR with IGF-II-specific primers spanning 200 bp located at the N terminus of the IGF-II coding region, glyceraldehyde-3-phosphate dehydrogenase (GAPDH), and ribosomal acidic phosphoprotein (RPLO) as described previously (18, 19). PCR products were subjected to electrophoresis on 2% agarose gels, and DNA was visualized by ethidium bromide staining.

In vivo tumor transplantation. The animal experimental protocols used in this study were approved by the Committee for Ethics of Animal Experimentation, and the experiments were conducted in accordance with the Guidelines for Animal Experiments in the National Cancer Center. To obtain nude mouse tumors, 5×10^6 cells were injected into the subcutaneous tissue of 6-week-old BALB/c nude mice (CLEA Japan, Inc.). Peritoneal dissemination of tumors was tested by injection of 4×10^6 44As3 or 5×10^6 NKPS cells suspended in 0.3 ml of RPMI 1640 medium into the peritoneal cavity. The mice were sacrificed 2 to 4 weeks after injection.

Immunohistochemistry and immunofluorescence. We obtained 10 paraffin-embedded tumor tissue samples of gastric scirrhous carcinoma in 2006 from the National Cancer Center Hospital. The study population consisted of five men (50%) and five women (50%). Paraffin blocks were sectioned into slices and subjected to immunohistochemical staining by the indirect polymer method with Envision reagent (Dako). Antigen retrieval was performed by placing sections in citrate buffer and heating them in a microwave pressure cooker according to the manufacturer's instructions. All sections were incubated with anti-C9orf10-C antibody (diluted 1:200).

UV cross-linking analysis. Cos1 cells were transfected with the indicated plasmids and extracted with a buffer containing 50 mM HEPES (pH 7.4), 0.1% NP-40, 140 mM KCl, 1 mM $MgCl_2$, 1% glycerol, and 1 mM EDTA (3). Extract was cleared at 14,000 × *g* for 10 min at 4°C, and the supernatant was used for the cross-linking assay. Cross-linking was performed in a binding buffer consisting of 10 mM HEPES (pH 7.4), 50 mM KCl, 3 mM $MgCl_2$, 5% glycerol, 1 mM dithiothreitol, and 100 μg/ml yeast tRNA. [^{32}P]UTP-labeled RNA transcripts with a specific amount or radioactivity (2×10^6 cpm) were incubated with 15 μg of Cos1 cells or 10 nM GST fusion protein for 30 min at room temperature. After UV cross-linking with UV-linker (FS-800; Funakoshi) for 4 min, the samples were treated with RNase A (0.5 mg/ml) at 37°C for 20 min and separated by SDS-PAGE. The gel was then dried and subjected to autoradiography.

RESULTS

Identification of C9orf10 as a tyrosine-phosphorylated protein binding to SFKs in gastric scirrhous carcinoma. To identify signaling molecules that mediate the progression of gastric scirrhous carcinoma cells in vivo, we analyzed the phosphotyrosine-containing proteins that bind to SFKs. We previously established human gastric scirrhous carcinoma cell line, 44As3, possessing a high potential for peritoneal dissemination in nude mice (Fig. 1A and B) (35). The histology of disseminated tumor nodules of 44As3 cells in the mouse peritoneal cavity reflects typical human gastric scirrhous carcinoma with the characteristics of scattered or loosely connecting cancer cells

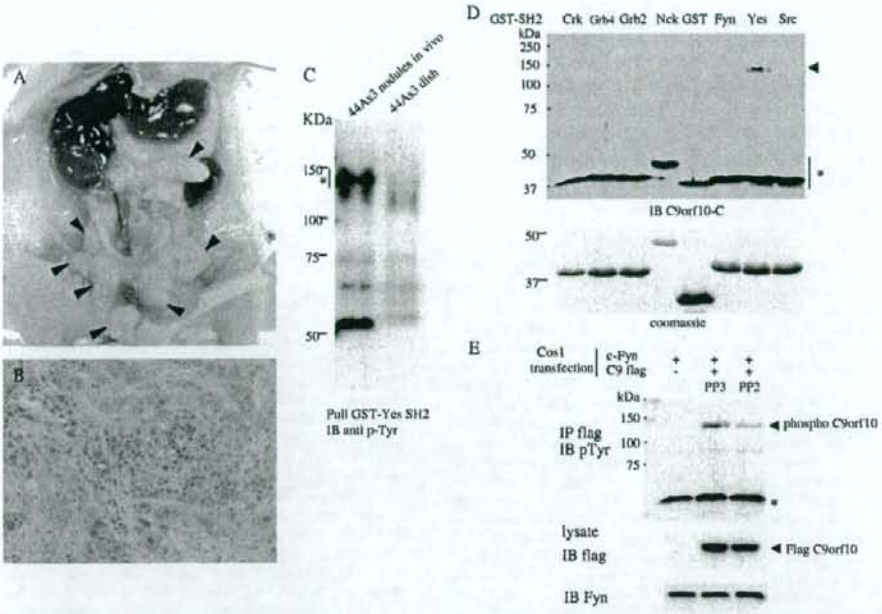

FIG. 1. Purification of tyrosine-phosphorylated proteins in tumor tissue of gastric scirrhous carcinoma. 44As3 cells (4×10^6/mouse) were transplanted into the peritoneal cavities of nude mice, and the mice were sacrificed 14 days later. (A) Peritoneal dissemination of 44As3 cells. Arrowheads indicate tumor nodules in the peritoneal cavity. (B) Histology of disseminated tumors of 44As3 cells. Hematoxylin-and-eosin staining was used. (C) Protein lysate prepared from disseminated tumor nodules of 44As3 cells or 44As3 cells cultured in a dish were purified with the SH2 domain of c-Yes. The eluted sample was separated by SDS-PAGE and immunoblotted (IB) with antiphosphotyrosine (4G10) antibody. The bands corresponding to the asterisk were excised from the gel and used for matrix-assisted laser desorption ionization–tandem mass spectrometry analysis. (D) The protein lysate of 44As3 cells was affinity precipitated with the GST-tagged SH2 domains of various adaptor proteins or SFKs as indicated above. The precipitates were subjected to immunoblotting with anti-C9orf10-C antibody, which reacts with the C terminus of C9orf10. The arrowhead indicates coprecipitated C9orf10. An asterisk indicates the cross-reaction of the antibody to GST fusion proteins. The GST fusion proteins used for pull-down were shown by Coomassie blue staining of the gel at the bottom. (E) Cos1 cells were cotransfected with C-terminally Flag-tagged C9orf10 and c-Fyn and treated with PP3 or PP2 (10 μM) before lysate preparation. C9orf10 was immunoprecipitated (IP), and the phosphorylation level was analyzed with 4G10. An asterisk indicates the heavy chain of immunoglobulin G.

with stromal fibrosis (Fig. 1B). Among c-Src, Fyn, and c-Yes, major SFKs in epithelial cells, the SH2 domain of c-Yes most effectively pulled down the tyrosine-phosphorylated proteins prepared from 44As3 tumor nodules disseminated in the peritoneal cavities of nude mice (data not shown). Within the proteins associated with c-Yes, proteins with molecular masses of 130 to 150 kDa were prominently phosphorylated in invasive tumor nodules compared with the usual tissue culture conditions (Fig. 1C). Therefore, the protein lysates of these 44As3 tumor nodules were sequentially purified with two affinity columns by using the c-Yes SH2 domain and anti-phosphotyrosine antibody 4G10; these 130- to 150-kDa bands were then cut out and analyzed by matrix-assisted laser desorption ionization–tandem mass spectrometry. In addition to several peptides corresponding to p130 Cas and CDCP1 (32, 33), two peptides were determined as parts of an uncharacterized protein called C9orf10. With a specific antibody against C9orf10, it was confirmed that c-Yes SH2 could actually pull down C9orf10 at the proper molecular weight, while the SH2 domain of the c-Src, Fyn, or SH2/SH3 adaptor protein could not (Fig. 1D). Tyrosine phosphorylation of C9orf10 was also observed in gastric cancer cells, which was effectively suppressed by treatment of cells with the SFK inhibitor PP2 (Fig. 1E).

To gain insight into the biological function of C9orf10, we next examined the intracellular distribution of C9orf10 with a polyclonal antibody generated against the carboxyl-terminal region of C9orf10. C9orf10 was abundantly expressed in the cytoplasm of the gastric cancer cells as fine granular staining (Fig. 2A). In some populations of the cells, C9orf10 also accumulated at the protruding cell edges (Fig. 2C). Such staining of C9orf10 was significantly reduced by treatment of cells with siRNA of C9orf10, and there was no signal by the control staining without the primary antibody (Fig. 2B and D).

Expression of C9orf10 was further examined in human gastric scirrhous cancer tissues by immunohistostaining. In normal gastric mucosa, weak cytoplasmic staining of C9orf10 was observed in the bottom region but not in the superficial region of the foveolar epithelium (Fig. 2 E and F). High-level expression of C9orf10 was clearly detected in gastric cancer cells invading the gastric wall (Fig. 2G). On the other hand, stromal cells such as fibroblasts, endothelial cells of veins, and muscle did not express C9orf10. No detectable signal was observed in the

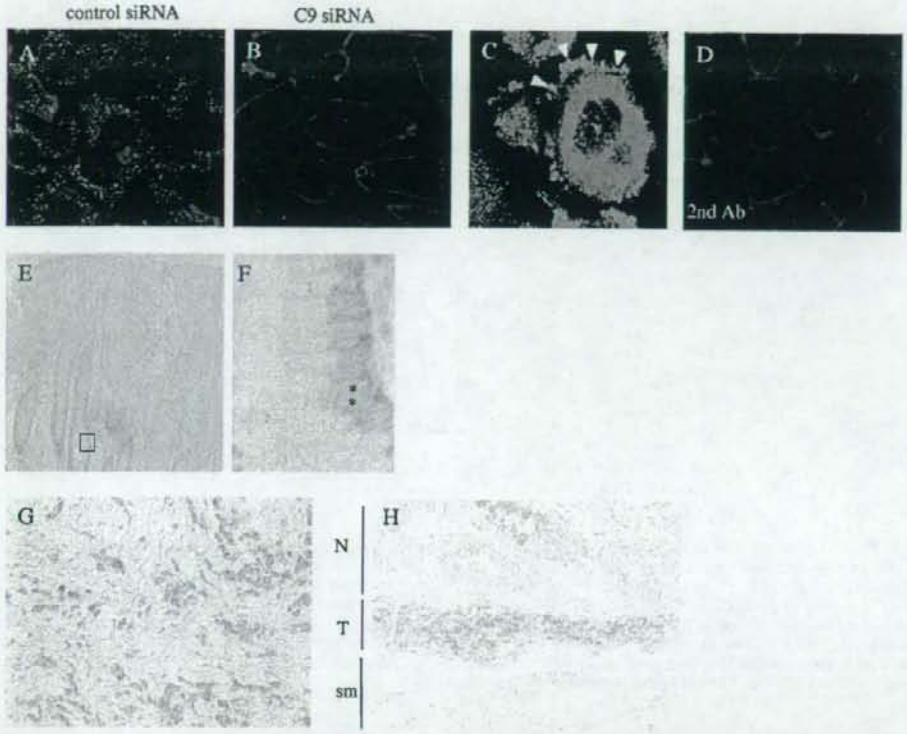

FIG. 2. Intracellular localization of C9orf10 and immunohistochemistry of C9orf10 in human gastric scirrhous carcinoma tissues. (A to D) 44As3 gastric cancer cells were treated with the control siRNA (A) or C9orf10 siRNA (B) or left untreated (C, D) and then immunostained with antibody raised against the C-terminal region of C9orf10 (C9orf10-C, green) and phalloidin (red). In panel D, cells were stained only with the secondary antibody (Ab) and phalloidin. Immunohistochemical staining of C9orf10 by anti-C9orf10-C antibody in noncancerous gastric mucosa (E, F) or gastric scirrhous carcinoma (G, H) is also shown. In normal mucosa, C9orf10 was detected in the bottom region of the foveolar epithelium. The square box in panel E is shown enlarged in panel F. The positions of nuclei are marked by asterisks. C9orf10 was diffusely stained in scirrhous cancer cells (G), and more intense staining was observed in cancer cells (T) compared to the normal mucosa (N) in panel H. sm, submucosal layer.

immunostaining of cancer cells with the second antibody alone (data not shown). Elevated expression of C9orf10 was observed in 70% of the scirrhous-type gastric cancer tissues (n = 10) compared with normal gastric mucosa, as shown in Fig. 2H.

C9orf10 physically interacts with SFKs and is a novel regulator of SFKs. The physical association between C9orf10 and SFKs was further examined by immunoprecipitation analysis. Although C9orf10 preferentially binds with the SH2 domain of c-Yes in vitro, C9orf10 was coimmunoprecipitated not only with c-Yes but also with Fyn and c-Src (Fig. 3A). C9orf10 was effectively pulled down by the SH3 domains of c-Src, Fyn, and c-Yes but not by the SH3 domain of cortactin, suggesting that the SH3 domains of SFKs are involved in the general association between C9orf10 and SFKs (Fig. 3B). From the analysis with truncated mutant forms of C9orf10, the region required for the interaction with the SH3 domain of Fyn was restricted to aa 339 to 405, which contains a polyproline motif (Fig. 3C). Similar results were obtained with GST-Src SH3 and GST-Yes SH3 (see Fig. S1A in the supplemental material). Coexpression of C9orf10 with c-Fyn in Cos1 cells caused marked tyrosine phosphorylation of C9orf10 (Fig. 3D). The specificity of c-Src, Fyn, and c-Yes for phosphorylation of C9orf10 was further examined in the SYF cell line, which is deficient in c-Src, Fyn, and c-Yes. When C9orf10 was coexpressed with individual SFKs, phosphorylation of C9orf10 was highly induced by Fyn and c-Yes and c-Src induced relatively weak phosphorylation of C9orf10 (see Fig. S1B in the supplemental material). These results indicate that C9orf10 associates with SFKs and is a novel substrate of SFKs.

Since several molecules have been reported to activate SFKs by association with the regulatory domain of SFKs, we next examined whether the expression of C9orf10 affects the activity of SFKs. The overexpression of C9orf10 increased the activity of SFKs in Hek293 cells, as judged by the antibody recognizing the phosphorylation of Tyr419 of SFKs, which recognizes c-Src, Fyn, c-Yes, Lyn, Lck, and Hck (Fig. 4A). SFK was also activated by expression of C-terminally truncated mutant C9orf10 N3, which possesses the region that binds SFKs, but

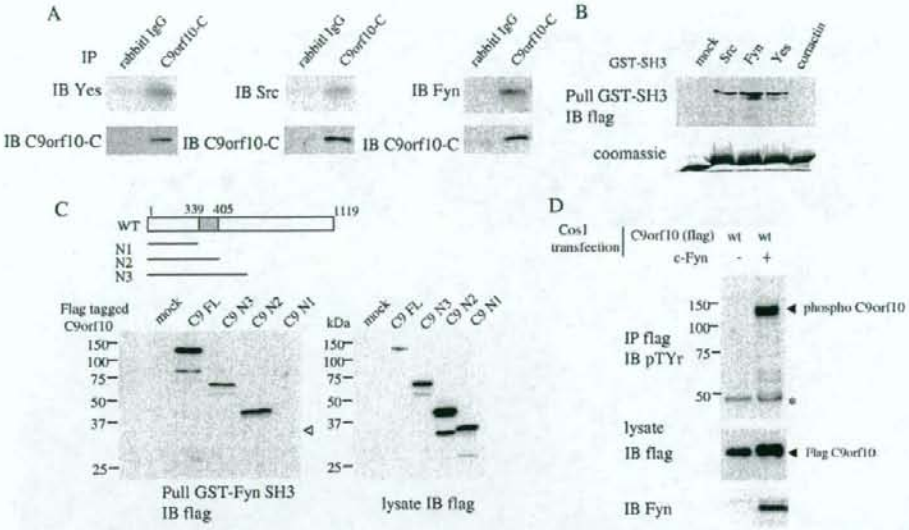

FIG. 3. Physical association of C9orf10 with SFKs. (A) Lysate of 44As3 cells was immunoprecipitated (IP) with anti-C9orf10-C antibody and immunoblotted (IB) with individual SFK antibody. Immunoprecipitated C9orf10 is shown at the bottom of each panel. IgG, immunoglobulin G. (B, C) Protein lysate of Cos1 cells transiently transfected with C-terminally Flag-tagged full-length (FL) C9orf10 or various deletion mutant forms (illustrated at the top of panel C) were pulled down with the GST-tagged SH3 domains of the indicated proteins (B) or GST-Fyn SH3 (C). The precipitates were immunoblotted with anti-Flag antibody. The expression of each C9orf10 construct in Cos1 cells is shown at the bottom right of panel C. The GST fusion proteins used for pull-down were revealed by Coomassie staining. WT, wild type. (D) Cos1 cells were transiently transfected with C-terminally Flag-tagged C9orf10 with or without c-Fyn. C9orf10 was immunoprecipitated with anti-Flag antibody, and its phosphorylation was detected by antiphosphotyrosine (4G10) antibody.

not by N1, which is unable to bind the SFK SH3 domain (Fig. 4B). Activation of SFKs in 44As3 cells by stably expressed C9orf10 was negated by treatment with C9orf10 siRNA (Fig. 4C). On the other hand, overexpression of C9orf10 did not affect the phosphorylation level of Tyr530, which negatively regulates SFK activity. These results indicate that C9orf10 is a novel activator of SFKs. Moreover, activation of c-Src, Fyn, and c-Yes by C9orf10 was individually examined in SYF cells. The coexpression of C9orf10 induced the activation of all three of these kinases. Although the proportion of the activated form of c-Src was relatively low, the relative increase in their activation by C9orf10 was almost the same (see Fig. S1C in the supplemental material).

C9orf10 is required for activation of the SFKs/PI3-kinase pathway to prevent oxidative stress-induced apoptosis. During the search for the biological function of the C9orf10 protein, we noticed that Akt was significantly activated in 44As3 cells stably expressing C9orf10, while only slight activation of Erk was detected (Fig. 4C). The activation of Akt was abolished by the treatment of cells with C9orf10 siRNA (Fig. 4C). These results indicate that Akt, which is one of the most significant proteins for the antiapoptotic function of cells, is involved in C9orf10-mediated signaling.

Oxidative stress caused by various cell stimuli such as UV irradiation or H_2O_2 treatment can lead to apoptotic cell death. We observed that the SFK inhibitor PP2 clearly increased apoptosis induced by exposure to UV in 44As3 cells or in another gastric scirrhous carcinoma cell line, NKPS. On the other hand, it did not affect the basal level of apoptosis of these cells under normal culture conditions (Fig. 5A). These results suggest an antiapoptotic effect of SFK activity in response to the oxidative stress.

Treatment of 44As3 cells with UV irradiation or H_2O_2 induced marked elevation of SFK activity, along with significant tyrosine phosphorylation of C9orf10 with a peak at 3 min and maintenance for 30 min (Fig. 5B; see Fig. S2A in the supplemental material). The activation of SFKs and phosphorylation of C9orf10 were dependent on the generation of ROS, because they were inhibited by the pretreatment of cells with *N*-acetylcysteine, a scavenger of ROS (Fig. 5C). Then we examined whether C9orf10 is required for the activation of SFKs as an antiapoptotic response to oxidative stress.

Reduction of endogenous C9orf10 expression by treatment of cells with siRNA clearly inhibited the activation of SFKs, Akt, and Erk caused by UV irradiation (Fig. 5D). We also observed that siRNA of C9orf10 blocks H_2O_2-induced activation of SFKs (see Fig. S2B in the supplemental material). At the same time, suppression of C9orf10 expression by 44As3 cells significantly enhanced apoptosis after treatment with UV irradiation or H_2O_2 (Fig. 5E, top; see Fig. S2C in the supplemental material). No significant change in apoptosis was caused by reduction of C9orf10 expression under normal culture conditions (Fig. 5E, top; see Fig. S1C in the supplemental material). On the other hand, overexpression of C9orf10 rescued cells from apoptosis after UV irradiation in Hek293 cells (Fig. 5E, middle). Importantly, mutant C9orf10 N1, which does

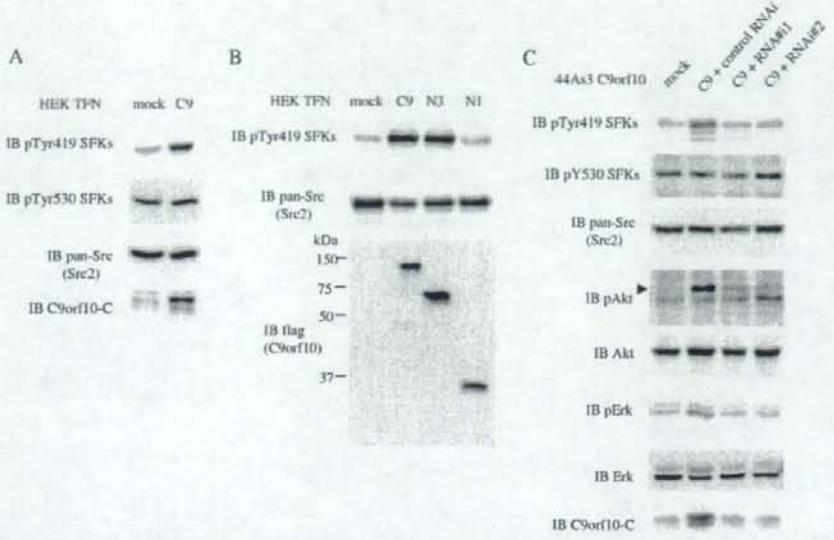

FIG. 4. Overexpression of C9orf10 activates SFKs and Akt. Hek293 cells (A, B) were transiently transfected with a control vector (mock), full-length C9orf10 (C9), or the deletion mutant forms tagged with Flag at the C terminus, as indicated. (C) 44As3 cells stably expressing C-terminally Flag-tagged C9orf10 were either treated with siRNAs of C9orf10 (RNA#i1, RNAi#2) or a control siRNA. The lysates were immunoblotted (IB) with the indicated antibodies. Anti-phospho-Src family antibody reacts with activated (pTyr419) or inactive (pTyr530) SFKs. Anti-pan-Src antibody (Src2) cross-reacts with Src, Fyn, Yes, and Fgr as also described in Materials and Methods.

not bind to SFKs, had no apoptosis-preventive effect (Fig. 5E, middle).

The SYF cell line was then used to examine whether the antiapoptotic function of C9orf10 exclusively depends on the activation of SFKs. Overexpression of C9orf10 in SYF cells did not affect apoptosis induced by UV irradiation, while it clearly rescued the apoptosis in $SYF^{+/+}$ cells, into which c-Src was stably reintroduced (Fig. 5E, bottom). Again, C9orf10 expression did not affect the basal level of apoptosis under normal culture conditions in SYF cells. Furthermore, coexpression of C9orf10 with c-Src more effectively rescued SYF cells from UV irradiation induced apoptosis (see Fig. S2D in the supplemental material). These results suggest that the antiapoptotic effect of C9orf10 depends on the activation of SFKs.

To understand the molecular mechanism of C9orf10-mediated Akt activation, we further examined whether C9orf10 mediates PI3-kinase activity through SFKs, as PI3-kinase is one of the major regulators of Akt. When the cells were treated with UV-C, the association of C9orf10 with SFKs or the p85 subunit of PI3-kinase was increased (Fig. 6A and B). The physical association of C9orf10 with p85 was abolished by the treatment of cells with PP2, suggesting that tyrosine phosphorylation of C9orf10 by SFKs is required for the association with p85 (Fig. 6B). It was also shown that the SH2 domain of p85 could efficiently pull down C9orf10 by affinity precipitation analysis (Fig. 6C). Marked tyrosine phosphorylation of p85 was induced by UV irradiation of cells and also abolished by treatment with PP2 (Fig. 6D). These results suggest that C9orf10 behaves as a scaffolding protein for p85 and SFK in response to UV irradiation, which leads to the phosphorylation and activation of PI3-kinase by SFK. The increased association of C9orf10 with SFK and PI3-kinase by UV irradiation was also suggested by the intracellular distribution of these proteins. C9orf10 is basically localized diffusely in the cytoplasm. UV irradiation causes the spreading of cells, and C9orf10 accumulates at the cell membrane, where SFKs are abundantly localized (Fig. 6E). Accumulation of C9orf10 in the nucleus to some extent was also observed (Fig. 6E). The distribution of p85 of PI3-kinase is similar to that of C9orf10, and membrane translocation of p85 was also observed after UV irradiation (Fig. 6F). A similar change in the intracellular localization of C9orf10 and p85 was observed in H_2O_2-treated cells (see Fig. S2E in the supplemental material). From these results, we designated C9orf10 Ossa for *O*xidative *s*tress-associated *S*rc *a*ctivator.

Ossa/C9orf10 is a novel RNA-binding protein and promotes the secretion of IGF-II. During the search for proteins that physically associate with Ossa, we noticed that Ossa associates with IMP-1 (unpublished data). It was later proved, however, that the association between Ossa and IMP-1 is RNA dependent (see Fig. S3 in the supplemental material). The RNA-binding activity of Ossa was thus examined by using synthetic ribonucleotide homopolymers. GST-fused proteins of three separate parts of Ossa were blotted onto a membrane and probed with ^{32}P-labeled RNA homopolymers. As shown in Fig. 7A, the carboxyl-terminal portion of Ossa (C9-C, aa 829 to 1119), but not the amino-terminal region (C9-N1, aa 1 to 338) or the middle part of Ossa (C9-M, aa 339 to 828), could directly bind to poly(U), as well as control IMP-1 KH domains

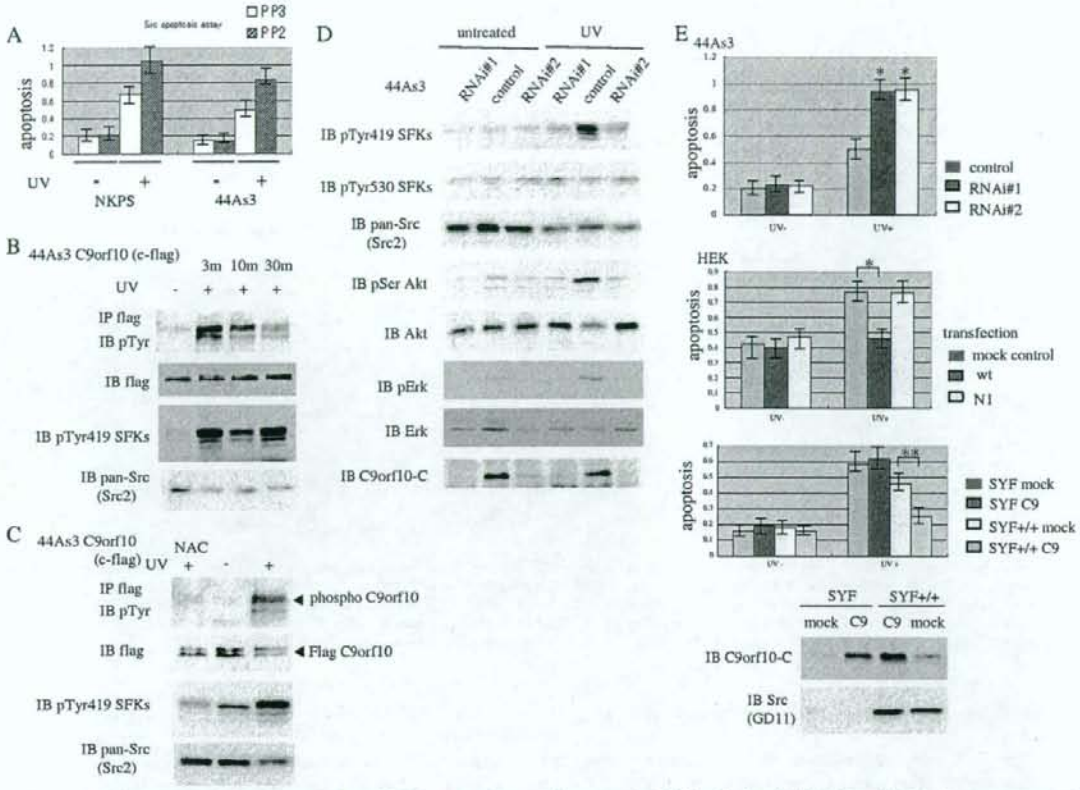

FIG. 5. C9orf10 is required for the activation of SFKs as an antiapoptotic response to UV irradiation. (A) NKPS or 44As3 cells were pretreated with PP3 or PP2 (10 μM). After the cells were irradiated with UV-C (40 mJ/cm^2), an apoptosis assay was performed. (B) 44As3 cells stably expressing C-terminally Flag-tagged C9orf10 (44As3 C9orf10) were treated with UV-C as in panel A and incubated for the indicated periods. The cells were lysed and subjected to immunoprecipitation (IP) of C9orf10 with anti-Flag antibody and immunoblotted (IB) with anti-phosphotyrosine antibody. The activation of SFKs was detected by antibody to pTyr419 SFKs. (C) 44As3 C9orf10 cells were treated with UV-C as in panel A and incubated for 3 min before lysis. In the left lane, cells were pretreated with *N*-acetylcysteine (10 mM) overnight before UV treatment. (D) 44As3 parent cells were treated with siRNAs of C9orf10 (RNAi#1 and RNAi#2) or the control scrambled siRNA (control) and irradiated with UV (40 mJ/cm^2). The lysate was immunoblotted with the antibodies indicated. (E) 44As3 parent cells were treated with siRNA as in panel D (top), Hek293 cells were transiently transfected with wild-type (wt) or deletion mutant C9orf10 (N1) tagged with Flag at the C terminus (middle), and C9orf10 was overexpressed in SYF cells or control SYF$^{+/+}$ cells by retrovirus infection (bottom). The cells were treated with UV irradiation (40 mJ/cm^2) and subjected to an apoptosis assay. The asterisks indicate differences from UV-irradiated control cells as follows: *, $P < 0.01$; **, $P < 0.05$.

(IMP-1 ΔN) (22). The Ossa C terminus could also bind poly(A) and poly(G) RNA homopolymers (data not shown).

Inspired by the association of Ossa with IMP-1 via RNA, we next checked the possibility that Ossa and IMP-1 directly bind to common mRNA targets such as IGF-II, which binds to IMP-1 (22). The binding of GST-tagged Ossa fragments with 6.0-kb IGF-II leader 3 mRNA (8) was examined by UV-cross-linking analysis. The signal for ^{32}P-labeled IGF-II mRNA was detected at the estimated location with the GST-fused carboxyl-terminal region of Ossa but not with any Ossa fragment which lacks the C-terminal region (Fig. 7B, left). The association between Ossa and IGF-II mRNA was disrupted in reaction mixtures containing IGF-II competitor RNA but not β-galactosidase competitor RNA (Fig. 7B, middle two panels), and Ossa did not bind to the coding region of β-galactosidase mRNA, which was used as a nonspecific control RNA (Fig. 7B, right). In addition, the coexpression of c-Fyn with Ossa in Cos1 cells did not alter the binding affinity of full-length Ossa for the IGF-II mRNA (Fig. 7C). These results indicate that the carboxyl terminus of Ossa, containing aa 829 to 1119, directly binds to IGF-II mRNA in a tyrosine phosphorylation-independent manner. Binding of Ossa with IGF-II mRNA was further demonstrated in vivo by detection of endogenous IGF-II mRNA in immunoprecipitate of epitope-tagged full-length Ossa but not Δ829-1119 Ossa from gastric cancer cell extracts (Fig. 7D). As controls, the same amount of nonspecific carry over of RNAs was observed in immunoprecipitates as detected by GAPDH and RPLO (Fig. 7D).

As RNA-binding proteins are reported to modify the translation of their target mRNAs, we next examined whether Ossa

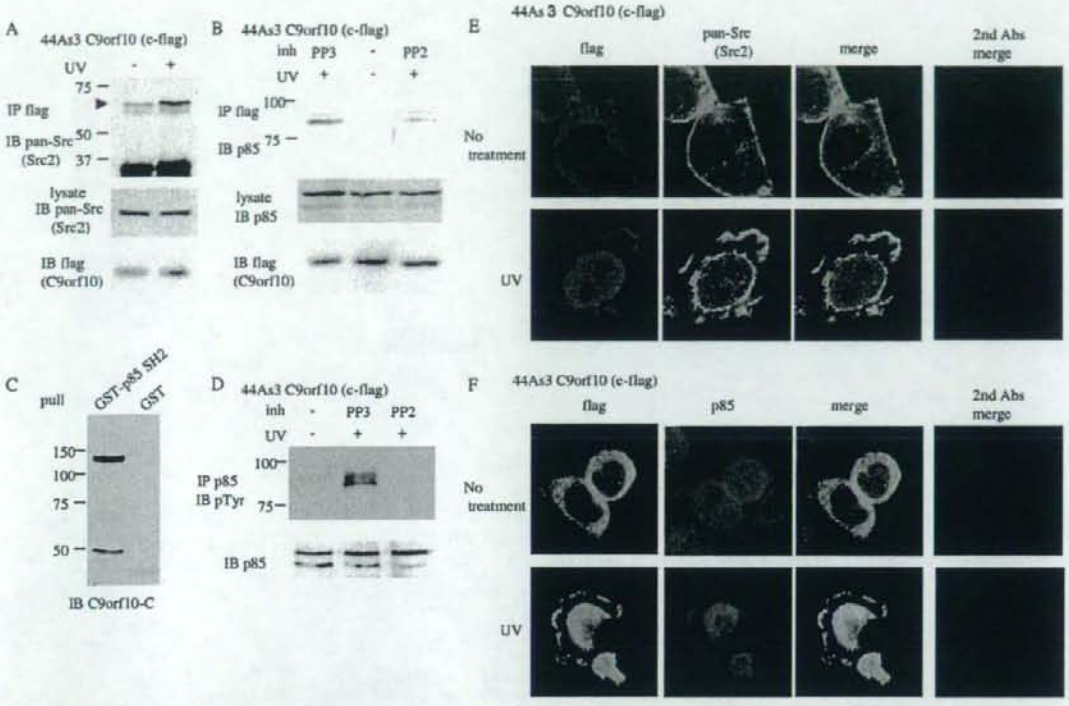

FIG. 6. Association of C9orf10 with SFKs and PI3-kinase. (A, B) 44As3 cells stably expressing Flag-tagged C9orf10 were left untreated or treated by UV irradiation (40 mJ/cm^2). In panel B, cells were pretreated with control PP3 or PP2 (10 μM) for 1 h before UV treatment. C9orf10 was immunoprecipitated (IP) with anti-Flag antibody, and coprecipitated SFKs or p85 was detected by immunoblotting (IB). (C) Protein lysate of 44As3 C9orf10 cells was pulled down with the GST-tagged SH2 domain of p85, and coprecipitated C9orf10 was detected by anti-C9orf10-C antibody. The band at 50 kDa is a nonspecific cross-reaction of the antibody. (D) 44As3 C9orf10 cells were treated with PP3 or PP2 and UV irradiated as in panel B. p85 of PI3-kinase was immunoprecipitated from the cells and immunoblotted with 4G10. (E, F) 44As3 C9orf10 cells left untreated or treated with UV-C (40 mJ/cm^2) were fixed 5 min after irradiation and immunostained with the antibodies indicated. Controls immunostained only with the secondary antibodies (Abs) are shown at right of each panel.

affects the production of IGF-II protein. When Ossa was overexpressed in gastric cancer cells, IGF-II protein in the culture medium was significantly increased; it was decreased to the basal level by reduction of Ossa expression from the same cells (Fig. 7E). The overexpression of the mutant form of Ossa which lacks the C-terminal region did not affect the extracellular secretion of IGF-II (Fig. 7E).

Suppression of Ossa/C9orf10 expression induced tumor apoptosis and blocked tumor invasion in nude mice. In order to analyze the effects of reduction of Ossa/C9orf10 expression on tumor formation and tumor invasion of gastric scirrhous carcinoma cells in vivo, we prepared 44As3 miOssa cells (stably expressing the microRNA for Ossa), which showed stable suppression of Ossa expression, by transducing the siRNA for Ossa with an RNAi expression vector system and selection in medium containing blasticidin (Fig. 8A, g). When 44As3 miOssa cells and control 44As3 miLacZ cells (stably expressing the microRNA for LacZ), into which a nonspecific siRNA for LacZ was introduced, were subcutaneously transplanted into 10 nude mice each, the tumor size was significantly reduced in miOssa cells compared to that in control miLacZ cells (Fig. 8A, a to e). Similar results were obtained from NKPS miOssa cells derived from gastric cancer cell line NKPS (data not shown). On the other hand, the proliferation of these cells under standard culture conditions was not significantly changed (Fig. 8A, f).

This reduction in tumor size may reflect an inhibition of growth and/or an increase in apoptosis of cancer cells in vivo. Therefore, the states of proliferation and apoptosis were individually examined in the tumor tissues. Subcutaneous tumor of 44As3 miOssa showed an increased level of apoptosis by analysis of TUNEL staining (Fig. 8B). The percentage of TUNEL staining-positive cancer cells was around 20% in the tumor of 44As3 miOssa cells and 3 to 4% in the tumor of 44As3 miLacZ cells. In contrast, there was no significant change in the level of Ki67, a marker of cell proliferation (Fig. 8C). These results indicate that Ossa might be suppressing tumor apoptosis during the progression of tumors in vivo.

The effect of Ossa on tumor invasion was also examined in vivo in an animal model of peritoneal dissemination. When control cells of 44As3 miLacZ or NKPS miLacZ were injected intraperitoneally into nude mice, severe carcinomatous perito-

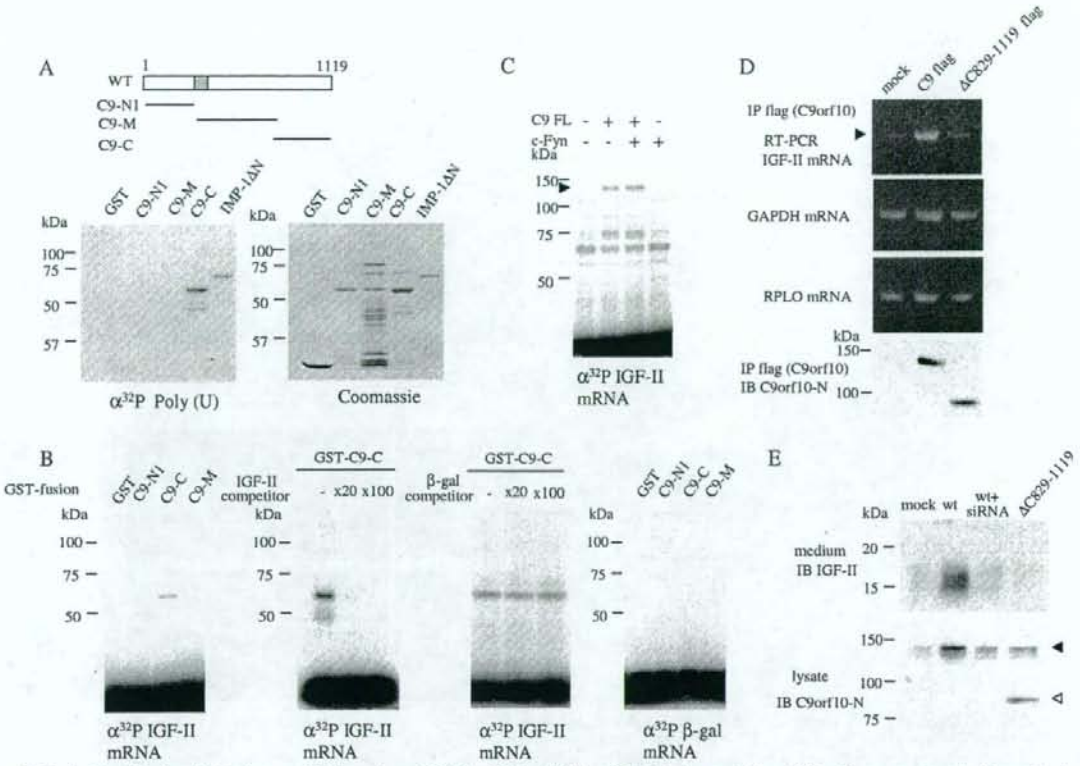

FIG. 7. C9orf10 directly binds to mRNAs such as IGF-II mRNA. (A) The RNA-binding activity of C9orf10 was analyzed with synthetic ribonucleotide homopolymers as probes. GST-fused IMP-1 and C9orf10 fragments were separated, transferred to polyvinylidene difluoride membranes, and incubated with ^{32}P-labeled poly(U). (Right bottom) Coomassie blue-stained gel showing each GST fusion protein. WT, wild type. (B, C) GST-fused C9orf10 fragments (B) or protein lysates prepared from Cos1 cells transfected with full-length (FL) C9orf10 with or without c-Fyn (C) were incubated with ^{32}P-labeled IGF-II leader 3 mRNA or the control mRNA of the β-galactosidase (β-gal) coding region. After UV cross-linking, samples were treated with RNase A and subjected to SDS-PAGE and autoradiography. The filled arrowhead in panel C indicates the position of full-length C9orf10. In panel B, unlabeled competitor of IGF-II or β-galactosidase as a nonspecific RNA was mixed with ^{32}P-labeled RNA. (D) Protein lysates prepared from 44As3 cells stably expressing full-length (C9) or truncated mutant C9orf10 (Δ829-1119) tagged with Flag at the C terminus or control mock vector-transfected 44As3 cells (mock) were immunoprecipitated (IP) with anti-Flag antibody in the presence of RNase inhibitors. RT-PCR of a 200-nucleotide IGF-II mRNA fragment, a 150-nucleotide GAPDH mRNA fragment, or a 103-nucleotide RPLO mRNA fragment was performed on the precipitated material. (E) Conditioned medium of NKPS cells stably expressing wild-type or truncated mutant C9orf10 was collected after the cells were incubated for 8 h in serum-free medium. Proteins secreted into the medium were precipitated with trichloroacetic acid (10%), resuspended in sample buffer, and subjected to immunoblotting (IB) with anti-IGF-II antibody. wt+siRNA, C9orf10-expressing NKPS cells treated with siRNA of C9orf10 before collection of the conditioned medium. The expression level of wild-type or mutant C9orf10 in each cell lysate is shown at the bottom with the antibody against the N terminus of the C9orf10 protein. Filled and open arrowheads indicate wild-type and Δ829-1119 mutant C9orf10, respectively.

nitis was observed, as previously described. Innumerable whitish nodules were observed in the mesentery and the surface of the liver of almost all of the mice injected with 44As3 miLacZ cells (n = 10, Fig. 8D; see Fig. S4 in the supplemental material). On the other hand, peritoneal dissemination of 44As3 miOssa cells was apparently modest. We did not observe dissemination of 44As3 miOssa cells on the liver surface, and tumor nodules in the mesentery were small and few (Fig. 8D; see Fig. S4 in the supplemental material). This reduction in tumor dissemination in the peritoneal cavity was also observed in NKPS miOssa cells (data not shown).

DISCUSSION

Exposure of cells to oxidative stress such as UV irradiation or H_2O_2 elicits a variety of responses. Severe oxidative stress leads to programmed cell death (7). On the other hand, oxidative stress also activates cell survival signaling, possibly by a protective response. For example, treatment of cells with UV irradiation or H_2O_2 induces the activation of Src by an unknown mechanism (1, 9, 11, 13). In this report, we demonstrate that Ossa/C9orf10 is a critical component of the oxidative stress-induced survival signaling through the activation of SFKs and PI3-kinase.

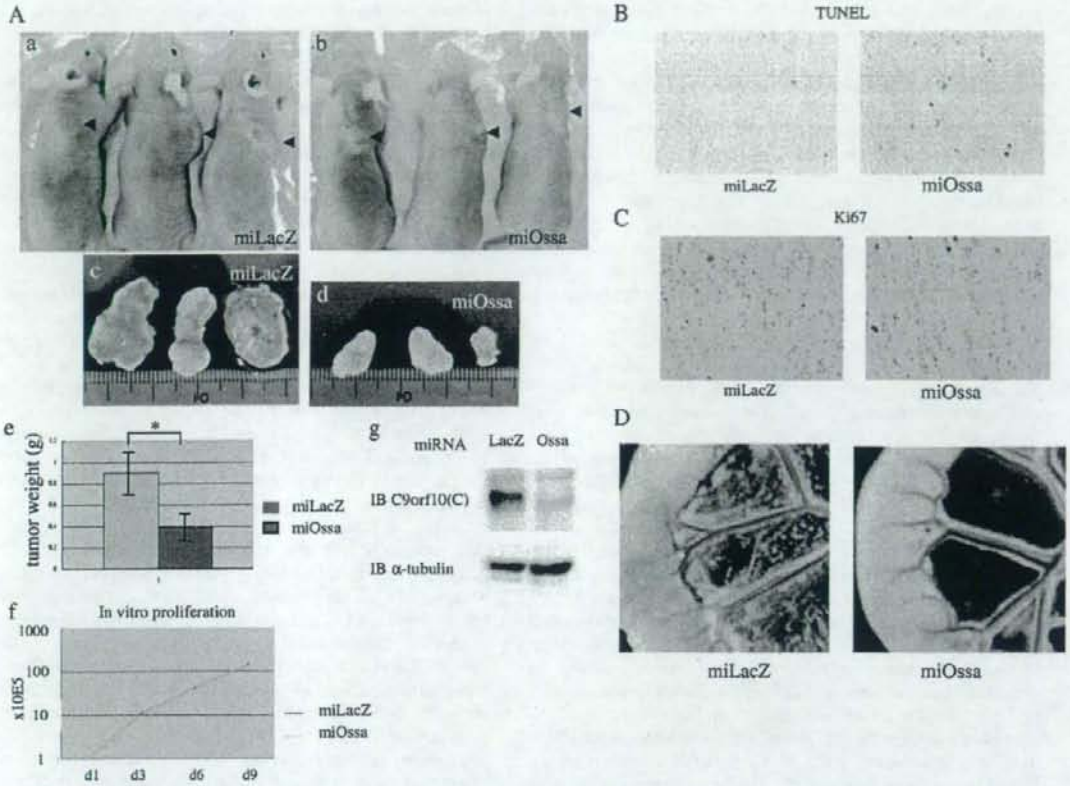

FIG. 8. Suppression of C9orf10 reduced tumor size in nude mice. (A) Control 44As3 miLacZ cells (a, c) or 44As3 miOssa cells (b, d) were injected subcutaneously into nude mice (5×10^6/mouse). The representative appearance of the mice (a, b) and excised tumors at 12 days after injection (c, d) is shown. (e) Average weight (± the standard deviation) of 10 tumors derived from either 44As3 miOssa or 44As3 miLacZ cells. (f) In vitro proliferation of 44As3 miOssa and miLacZ cells was evaluated by counting the cells under standard culture conditions. The experiments were performed twice in duplicate, and the mean cell number was plotted against time (days). (g) Expression level of C9orf10 in 44As3 miOssa or miLacZ cells. IB, immunoblotting. (B) TUNEL analysis of the tumors in panel A was performed as described in Materials and Methods. A total of 500 cancer cells of each tumor were scored for the ratio of TUNEL staining-positive cells. (C) Tumors from the nude mice in panel A were immunostained with anti-Ki-67 antibody. (D) 44As3 miOssa or miLacZ cells were injected intraperitoneally into mice (4×10^6/mouse), and the mice were sacrificed at 10 days after injection. The representative appearance of the dissected mesentery is shown.

The fate of cells exposed to oxidative stress depends on the balance between survival and apoptotic signaling. ROS-mediated DNA damage causes phosphorylation of ATM/ATR and p53, which leads to apoptosis (15, 17, 38). The time course of SFK activation, tyrosine phosphorylation of Ossa, and PI3-kinase activation was rapid, within 30 min of UV irradiation, which precedes the phosphorylation of ATM and p53 (see Fig. S5 in the supplemental material). Moreover, reduction of Ossa by siRNA did not affect the phosphorylation of p53 and ATM after lethal UV irradiation (data not shown). Therefore, Ossa-mediated activation of SFK and PI3-kinase seems to be a separate phenomenon from the p53-mediated signaling triggered by the DNA damage.

Ossa was identified in tumor nodules as a tyrosine-phosphorylated protein which binds to the c-Yes SH2 domain but not obviously to the SH2 domain of c-Src or Fyn. In addition, Ossa binds to the SH3 domain of all three SFKs and the relative increases in the activation of c-Src, Fyn, and c-Yes were almost the same. Therefore, it was suggested that the SH3 domain-mediated interaction of Ossa with SFKs may be critical for activation. Among the three SFKs, Ossa was highly phosphorylated by c-Yes and Fyn and relatively weakly phosphorylated by c-Src under the transient expression of the individual kinase in SYF cells (see Fig. S1B in the supplemental material). Although the effect of c-Src on Ossa phosphorylation was mild, it was enough to rescue the cells from apoptosis. As one of the reasons for the mild effect of c-Src on Ossa phosphorylation, the kinase activity of Src is relatively weak in the unstimulated condition (see Fig. S1C in the supplemental material).

Several cross talks between Src kinases and PI3-kinase have been suggested. We showed that Ossa functions as a scaffolding protein for SFK and PI3-kinase, which enables SFK to

phosphorylate and activate PI3-kinase. Such direct activation of PI3-kinase by SFK was supported by a previous report that incubation of purified p85/p110 with Src activated PI3-kinase activity in vitro (2). From this aspect, polyomavirus middle T also interacts with c-Src and activates its kinase activity that recruits PI3-kinase (10). As SFKs are also known to activate Akt through activation of the regulator of Akt such as 3-phosphoinositide-dependent protein kinases or PI3-kinase enhancer-activating Akt (31, 36), it is also possible that Ossa produces survival signaling via modification of these molecules. On the other hand, rapid activation of SFKs in response to oxidative stress does not depend on the RNA-binding activity of Ossa, as Ossa/C9orf10 N3, which lacks the mRNA-binding region, also activated SFKs (Fig. 4B).

As an early response to UV irradiation, Ossa is translocated to the cell membrane and tyrosine phosphorylated, which supports the idea that the cell survival function of Ossa is initiated at the cell membrane. Ossa has a hydrophobic amino acid stretch consisting of putative transmembrane domains; thus, Ossa may be recruited and tethered to the cell membrane (12). However, the molecular mechanism of the membrane recruitment of Ossa is not understood. A recent report suggests that cell surface membrane components such as G protein α subunits are directly activated by ROS, which contributes to Src activation (23). We cannot rule out the possibility that Ossa interacts with G protein and is recruited to the cell membrane, although treatment of cells with NF023, an antagonist of G protein α subunits, did not affect the membrane translocation of Ossa in response to UV irradiation (data not shown). In addition, direct activation of epidermal growth factor receptor or IGF receptor by UV irradiation or H_2O_2 treatment was recently demonstrated (4). Therefore, there is also a possibility that Ossa is involved in the RTK-mediated activation of the SFK/Akt pathway. Anyway, it is to be resolved further how oxidative stress triggers the rapid cellular response, including the translocation of Ossa. Upon treatment with Ossa siRNA, most of the cytoplasmic signal disappeared, suggesting a cytoplasmic localization of Ossa (Fig. 2A), although some signal remained, possibly caused by either remaining Ossa protein or nonspecific cross-reaction of the antibody.

Tumor cells are exposed to oxidative stress in various situations in vivo. Tumors rapidly outgrow their blood supply, leading to hypoxia, while tumors usually support their growth by stimulating angiogenesis. However, blood flow within the new vessels is often chaotic, causing periods of hypoxia followed by reperfusion. Such reperfusion causes the generation of ROS, which may therefore be a cause of oxidative stress within tumors (6, 24). In addition, tumors are frequently infiltrated by large numbers of macrophages, which have been shown to generate oxygen radicals (16). In addition, radiotherapy and photodynamic therapy generate oxygen radicals, and some chemotherapeutic agents such as cisplatin are also superoxide-generating agents (39). We observed increased expression of Ossa protein after the treatment of gastric cancer cells with cisplatin, suggesting some additional roles for Ossa in response to the chemotherapeutic agents (data not shown). Ossa may contribute to resistance to radiotherapy, photodynamic therapy, or chemotherapy by providing an antiapoptotic shield for cancer cells in these situations in vivo, which should be further elucidated by examination including the detection of tyrosine phosphorylation of Ossa in human cancer tissues after various clinical treatments.

We showed a distinct role for Ossa in the promotion of the extracellular secretion of IGF-II through the RNA-binding ability of the C-terminal region (aa 829 to 1119). Because many RNA-binding proteins function as translational regulators and control the protein level, Ossa may also affect the stability or translation of IGF-II mRNA, which increases the secretion of IGF-II. The human IGF-II gene contains four promoters, and each promoter drives the transcription of a distinct 5′ untranslated region (leader) that is spliced to the coding region (8). Ossa and IMP-1 bind to IGF-II leader 3 mRNA, which utilizes the major promoter in most tissues (8). Further experiments should be conducted to determine (i) whether Ossa and IMP-1 modify each other's functions and (ii) their biological significance in cancer progression. Elevated expression of IGF-II is often observed in human gastric cancer tissues, especially in the infiltrative-type cancers (29), and the paracrine or autocrine pathway of IGF-II causes a significant increase in the PI3-kinase and Akt pathway, which rescues cells from apoptosis (5). It was reported previously that cross talk occurs between SFKs and a factor that mediates nucleic acid-directed processes, a Src-associated substrate during mitosis, the 68-kDa protein Sam68, which belongs to the family of KH domain-containing RNA-binding proteins, and that its tyrosine phosphorylation via interaction with SFKs causes a decreased affinity for RNA (20, 21). On the other hand, the RNA-binding capacity of Ossa was not altered by phosphorylation via SFKs (Fig. 7C). Overall, the RNA-binding activity of the Ossa C-terminal region may be another mechanism to contribute to tumor growth and survival by the control of target mRNAs such as IGF-II mRNA.

Frequent overexpression of Ossa in gastric scirrhous carcinoma and the suppression of tumor growth by a decrease of Ossa in vivo suggest that Ossa may play a pivotal role in the progression of scirrhous-type gastric cancer. One of the critical functions of Ossa in cancer appears to be the support of cancer cell survival in environments with various oxidative stresses during cancer progression, invasion, and clinical treatments. The specific cellular signal mediated by the phosphorylation of Ossa is a promising therapeutic target of cancer progression and invasion.

ACKNOWLEDGMENTS

We thank J. Christiansen (University of Copenhagen) for donating plasmids encoding IGF-II leader 3 mRNA.

This work was supported by a Grant-in-Aid for Cancer Research from the Ministry of Education, Culture, Science and Technology of Japan and in part by a Grant-in-Aid from the Ministry of Health, Labor and Welfare of Japan for the third-term Comprehensive 10-year Strategy for Cancer Control.

REFERENCES

1. **Abe, J.-I., M. Takahashi, M. Ishida, J.-D. Lee, and B. C. Berk.** 1997. c-Src is required for oxidative stress-mediated activation of big mitogen-activated protein kinase 1 (BMK1). J. Biol. Chem. 272:20389–20394.
2. **Arcaro, A., M. Aubert, M. E. Espinosa, E. Hierro, U. K. Khanzada, S. Angelidou, T. D. Tetley, A. G. Bittermann , M. C. Frame, and M. J. Seckl.** 2007. Critical role for lipid raft-associated Src kinases in activation of PI3K-Akt signaling. Cell. Signal. 19:1081–1092.
3. **Atlas, R., L. Behar, E. Elliott, and I. Ginzburg.** 2004. The insulin-like growth factor mRNA binding-protein IMP-1 and the Ras-regulatory protein G3BP associate with tau mRNA and HuD protein in differentiated P19 neuronal cells. J. Neurochem. 89:613–626.

4. **Azar, Z. M., M. Z. Mehdi, and A. K. Srivastava.** 2006. Activation of insulin-like growth factor type-1 receptor is required for H_2O_2-induced PKB phosphorylation in vascular smooth muscle cells. Can. J. Physiol. Pharmacol. **84:**777–786.
5. **Brady, G., S. J. Crean, A. Lorenzon, and S. Kapas.** 2008. IGF-I protects human oral buccal mucosal epithelial cells from sodium nitroprusside-induced apoptosis via PI3-kinase. Growth Horm. IGF Res. **18:**298–306.
6. **Brown, N. S., and R. Bicknell.** 2001. Hypoxia and oxidative stress in breast cancer. Oxidative stress: its effects on the growth, metastatic potential and response to therapy of breast cancer. Breast Cancer Res. **3:**323–327.
7. **Cerutti, P. A., and B. F. Trump.** 1991. Inflammation and oxidative stress in carcinogenesis. Cancer Cells **3:**1–7.
8. **de Moor, C. H., M. Jansen, E. J. Bonte, A. A. M. Thomas, J. S. Sussenbach, and J. L. Van den Brande.** 1995. Proteins binding to the leader of the 6.0 kb mRNA of human insulin-like growth factor 2 influence translation. Biochem. J. **307:**225–231.
9. **Devary, Y., R. A. Gottlieb, T. Smeal, and M. Karin.** 1992. The mammalian ultraviolet response is triggered by activation of Src tyrosine kinase. Cell **71:**1081–1091.
10. **Dilworth, S. M.** 2002. Polyoma virus middle T antigen and its role in identifying cancer-related molecules. Nat. Rev. Cancer **2:**951–956.
11. **Griendling, K. K., D. Sorescu, B. Lassegue, and M. Ushio-Fukai.** 2000. Modulation of protein kinase activity and gene expression by reactive oxygen species and their roles in vascular physiology and pathophysiology. Arterioscler. Thromb. Vasc. Biol. **20:**2175–2183.
12. **Holden, S., and F. L. Raymond.** 2003. The human gene Cxorf17 encodes a member of a novel family of putative transmembrane proteins: cDNA cloning and characterization of Cxorf17 and its mouse ortholog orf34. Gene **318:**149–161.
13. **Kitagawa, D., S. Tanemura, S. Ohata, N Shimizu, J. Seo, G. Nishitai, T. Watanabe, K. Nakagawa, H. Kishimoto, T. Wada, T. Tezuka, T. Yamamoto, H. Nishina, and T. Katada.** 2002. Activation of extracellular signal-regulated kinase by ultraviolet is mediated through Src-dependent epidermal growth factor receptor phosphorylation. J. Biol. Chem. **277:**366–371.
14. **Kobayashi, Y., K. Suzuki, H. Kobayashi, S. Ohashi, K. Koike, M. Paolo, M. Kiebler, and K. Anzai.** 2008. C9orf10 protein, a novel protein component of Puro-containing mRNA-protein particles (Pur α-mRNPs): characterization of developmental and regional expressions in the mouse brain. J. Histochem. Cytochem. **56:**723–731.
15. **Kulms, D., and T. Schwarz.** 2002. Molecular mechanisms involved in UV-induced apoptotic cell death. Skin Pharmacol. Appl. Skin Physiol. **15:**342–347.
16. **Kundu, N., S. Zhang, and A. M. Fulton.** 1995. Sublethal oxidative stress inhibits tumor cell adhesion and enhances experimental metastasis of murine mammary carcinoma. Clin. Exp. Metastasis **13:**16–22.
17. **Lau, A. T. Y., Y. Wang, and J. F. Chiu.** 2008. Reactive oxygen species: current knowledge and applications in cancer research and therapeutic. J. Cell Biochem. **104:**657–667.
18. **Lemaire, F., R. Millon, J. Young, A. Cromer, C. Wasylyk, I. Schultz, D. Muller, P. Marchal, C. Zhao, D. Melle, L. Bracco, J. Abecassis, and B. Wasylyk.** 2003. Differential expression of head squamous cell carcinoma (HNSCC). Br. J. Cancer **89:**1940–1949.
19. **Liao, B., M. Patel, Y. Hu, S. Charles, D. J. Herrick, and G. Brewer.** 2004. Targeted knockdown of the RNA-binding protein CRD-BP promotes cell proliferation via an insulin-like growth factor II-dependent pathway in human K562 leukemia cells. J. Biol. Chem. **279:**48716–48724.
20. **Lukong, K. E., and S. Richard.** 2003. Sam68, the KH domain-containing superstar. Biochim. Biophys. Acta **1653:**73–86.
21. **Najib, S., C. Martin-Romero, C. Gonzalez-Yanes, and V. Sanchez-Margalet.** 2005. Role of Sam68 as an adaptor protein in signal transduction. Cell. Mol. Life Sci. **62:**36–43.
22. **Nielsen, J., J. Christiansen, J. Lykke-Andersen, A. H. Johnsen, U. M. Wewer, and F. C. Nielsen.** 1999. A family of insulin-like growth factor II mRNA-binding proteins represses translation in late development. Mol. Cell. Biol. **19:**1262–1270.
23. **Nishida, M., Y. Maruyama, R. Tanaka, K. Kontani, T. Nagao, and H. Kurose.** 2000. $G\alpha_i$ and $G\alpha_o$ are target proteins of reactive oxygen species. Nature **408:**492–495.
24. **Otani, H.** 2008. Ischemic preconditioning: from molecular mechanisms to therapeutic opportunities. Antioxid. Redox Signal. **10:**207–247.
25. **Ozben, T.** 2007. Oxidative stress and apoptosis: impact on cancer therapy. J. Pharm. Sci. **96:**2181–2194.
26. **Playford, M. P., and M. D. Schaller.** 2004. The interplay between Src and integrins in normal and tumor biology. Oncogene **23:**7928–7946.
27. **Portakal, O., O. Ozkaya, I. M. Erden, B. Bozan, M. Kosan, and I. Sayek.** 2000. Coenzyme Q10 concentrations and antioxidant status in tissues of breast cancer patients. Clin. Biochem. **33:**279–284.
28. **Shen, Y., G. Devgan, J. E. Darnell, Jr., and J. F. Bromberg.** 2001. Constitutively activated Stat3 protects fibroblasts from serum withdrawal and UV-induced apoptosis and antagonizes the proapoptotic effects of activated Stat1. Proc. Natl. Acad. Sci. USA **98:**1543–1548.
29. **Shiraishi, T., M. Mori, M. Yamagata, M. Haraguchi, H. Ueo, and K. Sugimachi.** 1998. Expression of insulin-like growth factor 2 mRNA in human gastric cancer. Int. J. Oncol. **13:**519–523.
30. **Sicheri, F., I. Moarefi, and J. Kuriyan.** 1997. Crystal structure of the Src family tyrosine kinase Hck. Nature **385:**602–609.
31. **Tang, X., Y. Feng, and K. Ye.** 2007. Src-family tyrosine kinase fyn phosphorylates phosphatidylinositol 3-kinase enhancer-activating Akt, preventing its apoptotic cleavage and promoting cell survival. Cell Death Differ. **14:**368–377.
32. **Uekita, T., L. Jia, M. Narisawa-Saito, J. Yokota, T. Kiyono, and R. Sakai.** 2007. CUB-domain containing protein 1 is a novel regulator of anoikis resistance in lung adenocarcinoma. Mol. Cell. Biol. **27:**7649–7660.
33. **Uekita, T., M. Tanaka, M. Takigahira, Y. Nakanishi, K. Yanagihara, and R. Sakai.** 2008. CUB-domain containing protein 1 regulates peritoneal dissemination of gastric scirrhous carcinoma. Am. J. Pathol. **172:**1729–1739.
34. **Ushio-Fukai, M., K. K. Griendling, P. L. Becker, L. Hilenski, and R. W. Alexander.** 2001. Epidermal growth factor receptor transactivation by angiotensin II requires reactive oxygen species in vascular smooth muscle cells. Arterioscler. Thromb. Vasc. Biol. **21:**489–495.
35. **Yanagihara, K., H. Tanaka, M. Takigahira, Y. Ino, Y. Yamaguchi, T. Toge, K. Sugano, and S. Hirohashi.** 2004. Establishment of two cell lines from human gastric scirrhous carcinoma that possess the potential to metastasize spontaneously in nude mice. Cancer Sci. **95:**575–582.
36. **Yang, K. J., S. Shin, L. Piao, E. Shin, Y. Li, K. A. Park, H. S. Byun, M. Won, J. Hong, G. R. Kweon, G. M. Hur, J. H. Seok, T. Chun, D. P. Brazil, B. A. Hemmings, and J. Park.** 2008. Regulation of 3-phosphoinositide-dependent protein kinase-1 (PDK1) by Src involves tyrosine phosphorylation of PDK1 and Src homology 2 domain binding. J. Biol. Chem. **283:**1480–1491.
37. **Yeatman, T. J.** 2004. A renaissance for Src. Nat. Rev. Cancer **4:**470–480.
38. **Yin, Y., G. Solomon, C. Deng, and J. C. Barrett.** 1999. Differential regulation of p21 by p53 and Rb in cellular response to oxidative stress. Mol. Carcinog. **24:**15–24.
39. **Yokomizo, A., M. Ono, H. Nanri, Y. Makino, T. Ohga, M. Wada, T. Okamoto, J. Yodoi, M. Kuwano, and K. Khono.** 1995. Cellular levels of thioredoxin associated with drug sensitivity to cisplatin, mitomycin C, doxorubicin, and etoposide. Cancer Res. **55:**4293–4296.

Oncogene (2009) 28, 662–673
 0950-9232/09 $32.00
www.nature.com/onc

ORIGINAL ARTICLE

Distinct role of ShcC docking protein in the differentiation of neuroblastoma

I Miyake[1], M Ohira[2], A Nakagawara[2] and R Sakai[1]

[1]*Growth Factor Division, National Cancer Center Research Institute, Tokyo, Japan and* [2]*Division of Biochemistry, Chiba Cancer Center Research Institute, Chiba, Japan*

The biological and clinical heterogeneity of neuroblastoma is closely associated with signaling pathways that control cellular characteristics such as proliferation, survival and differentiation. The Shc family of docking proteins is important in these pathways by mediating cellular signaling. In this study, we analysed the expression levels of ShcA and ShcC proteins in 46 neuroblastoma samples and showed that a significantly higher level of ShcC protein is observed in neuroblastomas with poor prognostic factors such as advanced stage and *MYCN* amplification ($P<0.005$), whereas the expression level of ShcA showed no significant association with these factors. Using TNB1 cells that express a high level of ShcC protein, it was demonstrated that knockdown of ShcC by RNAi caused elevation in the phosphorylation of ShcA, which resulted in sustained extracellular signal-regulated kinase activation and neurite outgrowth. The neurites induced by ShcC knockdown expressed several markers of neuronal differentiation suggesting that the expression of ShcC potentially has a function in inhibiting the differentiation of neuroblastoma cells. In addition, marked suppression of *in vivo* tumorigenicity of TNB1 cells in nude mice was observed by stable knockdown of ShcC protein. These findings indicate that ShcC is a therapeutic target that might induce differentiation in the aggressive type of neuroblastomas.
Oncogene (2009) **28,** 662–673; doi:10.1038/onc.2008.413; published online 10 November 2008

Keywords: Shc family; ERK; neuroblastoma; differentiation; RNAi

Introduction

Neuroblastoma is the most common pediatric solid tumor derived from the sympathoadrenal lineage of neural crest and its clinical and biological features are heterogeneous. Some types of neuroblastomas show favorable outcomes with spontaneous differentiation or regression by minimum treatment, whereas other types have malignant characteristics with metastasis and resistance to chemotherapy. Age of onset, tumor volume, presence of metastasis, pathological features and amplification of the *N-myc* gene are important prognostic factors of neuroblastoma. Previously, it was reported that the differential expression of Trk family receptors might contribute to clinical and biological outcomes of neuroblastomas (Nakagawara *et al.*, 1993; Nakagawara and Brodeur, 1997) whereas the cellular signaling involved in the regulation of the aggressiveness of neuroblastoma is largely unknown.

The Shc family of docking proteins is important in signaling pathways mediating the activation of various receptor tyrosine kinases (RTKs) such as the Trk family triggered by extracellular stimulations, to specific downstream molecules. The Ras–extracellular signal-regulated kinase (ERK) pathway and the phosphoinositide-3 kinase (PI3K)–Akt pathway are the most common signals regulated by Shc family proteins, representing important functions in cellular proliferation, survival and differentiation.

The Shc family has three members, ShcA/Shc, ShcB/Sli/Sck and ShcC/Rai/N-Shc encoded by different genes (Nakamura *et al.*, 1996; O'Bryan *et al.*, 1996; Pelicci *et al.*, 1996). ShcA protein having three protein isoforms, p46, p52 and p66, is ubiquitously expressed in most organs except the adult neural systems, whereas ShcC (p52 and p67 isoforms) are exclusively expressed in the neuronal system (Sakai *et al.*, 2000). In the central nervous system, ShcA expression is most significant during embryonic development with sudden decrease after birth. On the other hand, ShcC expression is remarkably induced around birth and maintained in the mature brain. The Shc family molecules have a unique PTB–CH1–SH2 modular organization with two phosphotyrosine-binding modules, PTB and SH2 domains, which recognize various phosphotyrosine-containing peptides with different specificities. CH1 domains contain several tyrosine phosphorylation sites that recruit other adaptor molecules such as Grb2. Functional analysis of ShcB and ShcC on the neuronal signal pathway indicate that these proteins in neuronal cells potentially regulate epidermal growth factor (EGF) or nerve growth factor (NGF) signaling in a similar fashion to ShcA (O'Bryan *et al.*, 1996; Nakamura *et al.*, 1998).

Major parts of neuroblastoma cell lines show the expression and tyrosine phosphorylation of ShcC protein, but its effect on the biology of tumor cells

Correspondence: Dr R Sakai, Growth factor Division, National Cancer Center Research Institute, Tsukiji, Chuo-ku, Tokyo 104-0045, Japan. E-mail: rsakai@ncc.go.jp
Received 9 May 2008; revised 3 September 2008; accepted 1 October 2008; published online 10 November 2008

remains to be elucidated. We have recently shown that constitutive tyrosine phosphorylation of ShcC is induced in a subset of neuroblastoma cells by the activation of anaplastic lymphoma kinase (ALK) owing to *ALK* gene amplification and the constitutively activated ALK–ShcC signal pathway could induce cell survival, anchorage-independent growth of the cells and progression of tumors (Miyake *et al*., 2002, 2005). In our study, significant amplification of *ALK* was observed in 3 of 13 neuroblastoma cell lines and in only 1 of 85 cases of human neuroblastoma samples (Osajima-Hakomori *et al*., 2005). Considering these results, it was suspected ShcC might also contribute to the signal pathway associated with the tumor behavior in ALK-independent manners in majority of neuroblastoma cells.

In a recent report, high expression of ShcC mRNA was shown to be a poor prognostic factor in neuroblastoma patients through the semiquantitative reverse transcriptase -PCR analysis of tissue samples (Terui *et al*., 2005), suggesting the possibility that ShcC protein might be causative of tumor progression in neuroblastoma patients. In the current study, we examined the expression levels of ShcC protein in tumor samples of 46 neuroblastoma patients and confirmed the significant association of the expression levels of ShcC protein with several factors linked to unfavorable outcome of neuroblastoma. Furthermore, we investigated the functions of ShcC in cell proliferation, differentiation and *in vivo* tumorigenicity of neuroblastoma cells by knockdown of ShcC expression in neuroblastoma cell lines expressing a high level of ShcC without *ALK* amplification.

Results

Expression and tyrosine phosphorylation of ShcC in neuroblastoma cell lines

At first, the expression of ShcA and ShcC was analysed in 11 neuroblastoma cell lines using each specific antibody (Supplementary Figure A) along with DLD-1 as a control, which is known to express ShcA protein (mainly p46ShcA and p52ShcA), but not ShcC protein (Figure 1a). The three cell lines with *ALK* gene amplification (NB-39-v, Nagai and NB-1: Group A) expressed ShcC at a moderate level in contrast to their significant phosphorylation so that ALK–ShcC complex is mediating the dominant oncogenic signal (Miyake *et al*., 2002; Osajima-Hakomori *et al*., 2005). Other

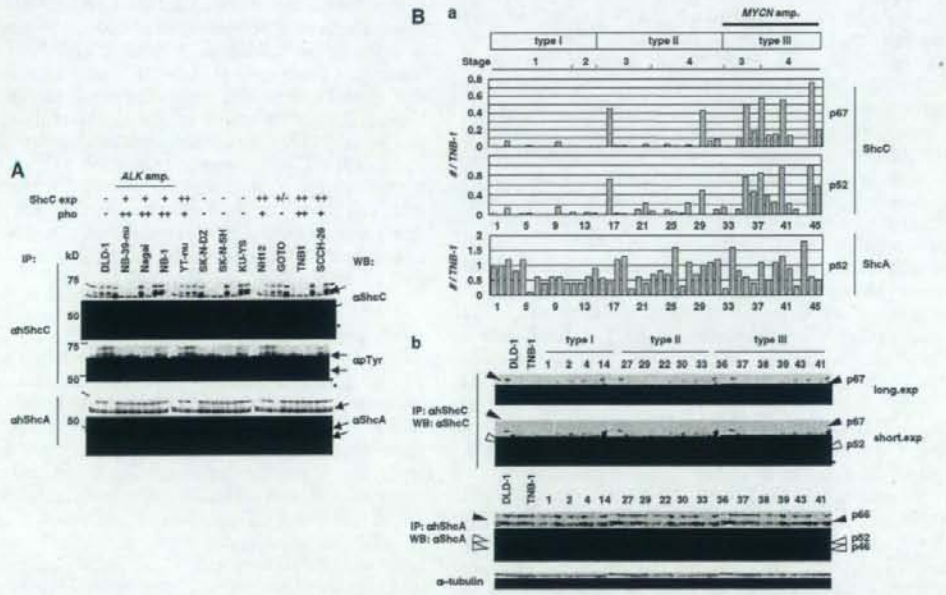

Figure 1 (**A**) Expression and tyrosine phosphorylation of ShcC in neuroblastoma cell lines detected by specific antibody. The expression of ShcA (lower panel), ShcC (upper panel) and tyrosine phosphorylation of ShcC was analysed in 11 neuroblastoma cell lines including the cell lines with anaplastic lymphoma kinase (*ALK*) gene amplification (*ALK* amp.) along with DLD-1 as a control. Lysates were immunoprecipitated and then immunoblotted with antibodies against the indicated molecules. The levels of expression/phosphorylation of ShcC are indicated above. Asterisks show heavy chains of immunoglobulin. Positions of molecular mass markers (kDa) are shown to the left. (**B**) Expression of ShcC and ShcA in the tissue samples of three subsets of neuroblastoma patients. (a) Expression levels of ShcC/ShcA in the samples of 46 neuroblastoma patients were detected by western blotting being compared to the level of expression in TNB-1 cells (= 1.0) as an internal control among each experiment and was corrected by each expression level of a-tubulin. (b) Expression of ShcC (upper panel)/ShcA (middle panel) of representative samples of each subset were detected on a filter. The exposure time of the filter onto X-ray films was different to detect between p52ShcC (short exposure: lower panel) and p67ShcC (long exposure: upper panel). Each isoform of ShcC/ShcA is indicated by opened or filled triangles. Asterisks show heavy chains of immunoglobulin.

neuroblastoma cells with a single copy of the *ALK* gene were divided into two groups, one with considerably high levels of ShcC expression (YT-v, NH-12, TNB-1 and SCCH-26: Group B) and the other with almost no ShcC expression (KU-YS, SK-N-DZ, SK-N-SH and GOTO: Group C). Most of the cells in the Group B showed a morphological tendency to aggregate each other and rather low adhesion to the culture plate, compared with the cells of the Group C (data not shown). The degrees of ShcC phosphorylation in the cells in Group B appeared to be lower than the cells with *ALK* amplification (Figure 1A, middle panel). In contrast to ShcC, the expression of ShcA was within similar levels among neuroblastoma cell lines (Figure 1A, lower panel).

The expression level of ShcC is prominent in tissue samples of poor risk neuroblastoma patients

Next we analysed the expression of ShcA and ShcC protein in 46 primary human neuroblastoma specimens using each specific antibody. These tissue samples were classified into three subsets using Brodeur's classification; type I (stage 1, 2 or 4S; a single copy of *MYCN*), type II (stage 3 or 4; a single copy of *MYCN*) and type III (all stages; amplification of *MYCN*) (Brodeur and Nakagawara, 1992; Ohira *et al*., 2003). The expression level of ShcA and ShcC in western blotting was standardized by intensity of α-tubulin within each filter, standardized by the amounts in TNB-1 cells as an internal control among different filters and statistically evaluated from at least two independent western blots for each sample (Table 1). We found that there is a significant difference in the expression levels of ShcC among the subsets of neuroblastomas. In the group of type II and type III, the expression level of ShcC protein was substantially higher than that in the type I group (Figure 1Ba). Both isoforms of ShcC, p52ShcC and p67ShcC, showed similar patterns of expression. As shown in Table 2, the expression level of ShcC has a significant correlation with several clinical factors including late onset of the disease (later than 12 months) (p52/p67: $P<0.001/P=0.015$), advanced clinical stage (stages III and IV) ($P<0.001$) and gene amplification of *MYCN* (p52/p67: $P<0.002/P=0.005$). Furthermore, most of the samples from the patients who died within 12 months after the onset of the disease showed significantly higher levels of ShcC expression than the other group of samples in which patients lived longer than 12 months (p52/p67: $P=0.006/P=0.009$). In contrast, variable expression levels of both isoforms of ShcA protein, p52 and p66, were observed in neuroblastoma samples with no significant difference among three subsets of clinical group ($P>0.05$) (Table 2; Figure 1Ba). The results of representative samples from each subset are shown in Figure 1Bb. These data indicate that the expression of ShcC protein is significantly associated with multiple prognostic factors of neuroblastoma, suggesting that ShcC has specific functions in malignant phenotypes of neuroblastoma presumably by modulating cellular signaling.

Biological effects of ShcC downregulation on TNB-1 cells

To elucidate the biological functions of ShcC in the tumor characteristics causing unfavorable outcomes of neuroblastoma patients, we investigated the effects of ShcC knockdown on the cellular biology and signal transduction in one of the neuroblastoma cell lines, TNB-1, which expresses a high level of ShcC protein with no *ALK* amplification. The expression of ShcC and ShcA was suppressed by RNA interference using two independent sets of specific small interfering RNA (siRNA) oligonucleotides corresponding to ShcC and ShcA, respectively (Figure 2Aa). The growth rate of TNB-1 cells transfected with the ShcA siRNA was severely suppressed (Figure 2Ab), owing to impaired ability of proliferation and survival, which is consistent with previous reports (Ravichandran, 2001). ShcC-knockdown cells showed a relatively weak effect on growth rate in the normal culture condition (Figure 2Ab).

Downregulation of ShcC induces neurite outgrowth and increases differentiation-related markers in TNB-1 cells

ShcC knockdown caused morphological changes to rather flat and spindle shape and neurite extension within 24 h after transfection of ShcC siRNA (Figure 2Ba). These neurite-bearing cells express higher amount of microtubule-associated protein 2 (MAP-2), growth-associated protein 43 (GAP-43), a protein expressed in the growing neurites, and chromogranin A (Chr-A; Figure 2Bb), markers of neuronal differentiation (Giudici *et al*., 1992) than the control cells. On the other hand, TNB-1 cells treated with ShcA siRNAs showed no remarkable change compared with the control cells, relatively round with small processes attached to the dish surface (Figure 2Ba). These results suggest that the endogenous ShcC negatively affects neurite outgrowth and differentiation of TNB-1 cells.

Persistent activation of ERK1/2 due to ShcC downregulation induces neurite outgrowth in TNB-1 cells

Neuronal differentiation is closely associated with mitogen-activated protein kinase (MAPK)/ERK kinase (MEK)/ERK and PI3K–AKT pathways and both of them might be controlled downstream of Shc family signaling. Downregulation of ShcA induced the suppression of extracellular signal-related kinase 1/2 (ERK1/2) and AKT pathways at 48 h after transfection of siRNA, nevertheless ShcC downregulation apparently elevated the base level of ERK phosphorylation and slightly enhanced AKT activation (Figure 3a). This elevation of ERK phosphorylation sustained until 96 h after transfection of siRNA. Similar effect on the ERK activation was also observed in NH-12 and YT-v cells, which express high amount of ShcC (Supplementary Figure B). It is reported that sustained activation of ERK is responsible for neurite outgrowth and differentiation of PC12 cells (Qui and Green, 1992). To investigate whether neuronal extension of TNB-1 cells by ShcC RNAi was induced by sustained activation of ERK, the effect of MEK inhibitor, PD98059, on the

Table 1 Characteristics of 46 neuroblastoma samples

Case	*Type*	*Stage*	*Age (months)*	*MYCN*	*Prognosis*	*p52ShcC*	*p67ShcC*	*p52ShcA*	*p66ShcA*
1	I	1	8	1	A	0.01	0	0.92	0.58
2		1	7	1	A	0	0	0.92	0.52
3		1	8	1	A	0.13	0.07	1.16	0.58
4		1	1	1	A	0	0	0.81	0.63
5		1	4	1	A	0.013	0	1.26	0.62
6		1	8	1	A	0.03	0.006	0.81	0.60
7		1	8	1	A	0	0	0.54	0.70
8		1	7	1	A	0	0	0.40	0.48
9		1	9	1	A	0	0	0.40	0.58
10		1	7	1	A	0.15	0.05	0.42	0.31
11		1	7	1	A	0.003	0	0.35	0.36
12		2	38	1	A	0.047	0	0.41	0.20
13		2	7	1	A	0	0	0.40	0.39
14		2	7	1	A	0.038	0	0.60	0.63
15		2	>132	1	A	0.03	0	0.83	0.62
16	II	3	8	1	A	0	0	0.56	0.45
17		3	7	1	A	0.72	0.45	0.42	0.49
18		3	7	1	A	0.03	0.01	1.2	0.62
19		3	8	1	A	0.015	0.01	1.3	0.67
20		3	23	1	A	0	0	0.25	0.32
21		3	22	1	A	0.10	0	0.63	0.63
22		3	>108	1	A	0.23	0.03	0.45	0.36
23		3	18	1	A	0.074	0.025	0.75	0.45
24		3	47	1	A*	0	0.03	0.87	0.65
25		3	21	1	D	0.089	0.03	0.76	0.56
26		3	96	1	A*	0.054	0.001	1.6	0.54
27		4	5	1	A	0.03	0	1.03	0.28
28		4	55	1	A	0.22	0.018	1.14	0.33
29		4	4	1	A	0	0	0.52	0.49
30		4	22	1	D	0.49	0.43	0.89	0.48
31		4	45	1	A*	0	0.068	1.17	0.53
32		4	57	1	A*	0.10	0.093	1.2	0.42
33		4	102	1	A*	0.15	0	1.5	0.49
34	III	3	32	amp	A*	0	0	1.6	0.37
35		3	13	amp	D	0.11	0.10	0.86	0.53
36		3	33	amp	D	0.77	0.50	0.64	0.50
37		3	21	amp	A*	0.47	0.18	0.47	0.49
38		3	26	amp	A*	0.84	0.57	1.1	0.58
39		4	23	amp	D	0.38	0.13	0.99	0.35
40		4	7	amp	D	0.25	0.15	1.1	0.58
41		4	>132	amp	D	0.96	0.55	1.32	0.65
42		4	18	amp	D	0.22	0.13	0.99	0.63
43		4	>24	amp	D	0.10	0	0.76	0.54
44		4	59	amp	D	0	0	1.80	0.85
45		4	30	amp	D	0.99	0.76	0.60	0.56
46		4	34	amp	D	0.56	0.21	0.53	0.47

Type, as described in 'Materials and methods'; age: onset of the disease (months); stage, INSS stage; MYCN, single copy (1) or amplification (amp) of *MYCN* gene; prognosis, alive (A) or death (D) within 12 months after diagnosis; A*, death after 12 months from diagnosis; p52/p67 ShcC and p52/66 ShcA, the intensity of each band obtained by western analysis, standardized according to control signals, such as the bands of TNB-1 and α-tubulin as described in 'Materials and methods'.

differentiation of TNB-1 cells by knockdown of ShcC was examined. It was found that inhibition of the ERK pathway abolished the neurite outgrowth of TNB-1 cells by ShcC knockdown, indicating that ShcC protein has the potential to suppress neurite outgrowth which is dependent on the sustained activation of the ERK pathway (Figure 3b). In addition, the sustained activation of ERK by the expression of activated Raf protein, RafCAAX (Leevers *et al*., 1994; Stokoe *et al*., 1994) also induced neurite outgrowth in TNB-1 cells (Supplementary Figure C) just as in PC12 cells (Dhillon *et al*., 2003). We also analysed the effect of PI3K inhibitor on neurite outgrowth induced by ShcC RNAi to check the involvement of the PI3K–AKT pathway, whereas no apparent effects on the number and length of the neurite extension were observed (Supplementary Figure D).

Effect of ShcC knockdown on ERK activation is enhanced by collagen stimulation by ShcA–Grb2 signaling

Among several culture conditions of cells examined for the effect of ShcC RNAi on the activity of ERK, the most obvious activation of ERK was observed after the

Table 2 Correlation between the expression of ShcC protein and identified prognostic factors of neuroblastoma

	p52		*p67*	
	Average	*t-Test*	*Average*	*t-Test*
ShcC				
Age (months)				
12>	0.071		0.037	
>12	0.27	**<0.001**	0.18	0.015
Stage				
I–II	0.03		0.0084	
III–IV	0.26	**<0.001**	0.14	**<0.001**
MYCN				
Single	0.083		0.040	
amp.	0.43	**0.002**	0.25	**0.005**
Death in 12 months				
–	0.10		0.047	
+	0.41	**0.006**	0.25	**0.009**
	p52		*p66*	
	Average	*t-Test*	*Average*	*t-Test*
ShcA				
Age (months)				
12>	0.72		0.53	
>12	0.82	0.2	0.52	0.32
Stage				
I–II	0.68		0.52	
III–IV	0.82	0.1	0.52	0.22
MYCN				
Single	0.73		0.51	
amp.	0.88	0.16	0.55	0.16
Death in 12 months				
–	0.75		0.50	
+	0.84	0.27	0.57	0.11

Expression levels of ShcC and ShcA in tissue samples from 46 neuroblastoma patients quantified were analyzed statistically using *t*-test. The variables compared are age, onset of the disease (months); stage, INSS stage; MYCN, single copy or amplification of *MYCN* gene. Statistically significant correlation ($P<0.01$) is indicated in bold.

cells were plated on collagen dishes following suspending condition (Figure 4a, lower panel). On the contrary, the activation level of ERK due to ShcC RNAi was not significant in the suspending condition (Supplementary Figure E, left panel) showing that ShcC RNAi-induced ERK activation depends on attachment to the specific extracellular matrix (ECM).

In contrast, ERK activation was consistently suppressed by knockdown of ShcA regardless of these culture conditions (Figure 4a, upper panel).

Integrins-mediated extracellular signaling lead the activation of Ras/ERK signaling by ShcA, and that process is reported to be associated with Src family kinase (Wary *et al*., 1996, 1998), focal adhesion kinase (Hecker *et al*., 2002) or some RTKs (Moro *et al*., 1998; Hinsby *et al*., 2004). In TNB-1 cells, enhanced ShcA phosphorylation and ShcA–Grb2 complex formation was observed following collagen stimulation and further increased by ShcC RNAi (Figures 4b and c). To examine whether the phosphorylation of ShcA is necessary for the neurite formation, the effect of double knockdown of both ShcC and ShcA was examined in TNB-1 cells. ERK activation and neurite outgrowth were not detected in the absence of both ShcC and ShcA, indicating that ShcC RNAi-induced neurite outgrowth of TNB-1 cells might be dependent on the ShcA expression in adherent state (Figure 4d).

Expression of ShcC suppresses the phosphorylation of ShcA in KU-YS cells stimulated by EGF

To further analyse the effects of ShcC expression on ShcA phosphorylation in neuroblastoma cells, we introduced a vector expressing p52ShcC into KU-YS neuroblastoma cells, which do not express a detectable amount of endogenous ShcC protein (Figure 1A), and obtained several stable clones expressing p52ShcC at different levels (Figure 5a). As controls, clones overexpressing p46/p52ShcA, or expressing the expression vector alone were also prepared. We checked the ShcA phosphorylation of each clone under the stimulation of EGF (Figure 5b). EGF stimulation to the control and ShcA expressing cells showed typical activation of ShcA, whereas the cell expressing ShcC showed decreased levels of ShcA phosphorylation according to the levels of ShcC protein. We also confirmed that activation of ShcA by EGF was suppressed in the cells transiently overexpressing ShcC (Supplementary Figure F). Those cells showed almost the same level of EGF receptor (EGFR) activation induced by EGF, judging from the phosphorylation levels of EGFR indicating that the expression of ShcC negatively affected the EGFR–ShcA signaling after the activation of EGFR, such as competing manners against ShcA. In addition, we examined whether tyrosine phosphorylation of ShcC is crucial for the suppression of ShcA phosphorylation by establishing two clones that express a p52ShcC mutant, 3YF lacking all three tyrosines, which are reported to be involved in the tyrosine phosphorylation of ShcC (Miyake *et al*., 2005). It was revealed that the 3YF mutant of ShcC could suppress the EGF-induced activation of ShcA in both clones almost as efficiently as the original ShcC in ShcC2 cells (Supplementary Figure G), suggesting that negative regulation of ShcA phosphorylation by ShcC does not require tyrosine phosphorylation of ShcC.

ShcC downregulation negatively affects anchorage-independent growth and in vivo *tumorigenicity*

We investigated the effect of ShcC knockdown on the anchorage-independent growth and *in vivo* tumorigenicity of TNB-1 cells by establishing cells with stable suppression of ShcC expression using the miR RNAi expression vector (as described in 'Materials and methods'). As analysed in the mixed clones by soft agar colony formation assay, stable suppression of ShcC caused marked inhibition of anchorage-independent growth (Figure 6a). Three isolated clones of ShcC miR

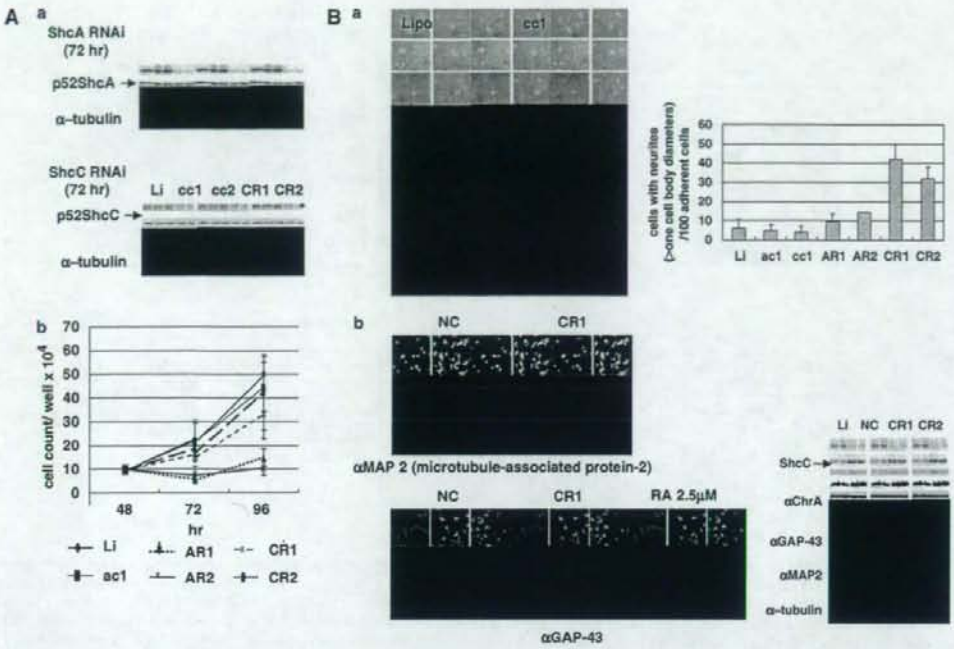

Figure 2 Biological effects of ShcC downregulation using small interfering RNA (siRNA) on TNB-1 cells. (**A**) (a) Expression of ShcC (lower panel) and ShcA (upper panel) was suppressed by RNA interference using specific siRNA oligonucleotides corresponding to ShcC and ShcA, respectively, then, detected by western analysis with each specific antibody. (b) Growth rate of siRNA-treated cells in tissue culture condition. TNB-1 cells 48 h after the transfection with ShcA/ShcC siRNA cultured by 30-mm dishes were counted at the indicated time points. The results represent the average values (± s.d.) of three replicated experiments. (**B**) Downregulation of ShcC induces neurite outgrowth and increases the expression of differentiation-related markers in TNB-1 cells. (a) Evaluation of neurite outgrowth of ShcA or ShcC-knockdown TNB-1 cells 72 h after siRNA treatment without any extracellular matrix (ECM) stimulation. (b) Expression of several molecules used as differentiation-related markers in ShcC-knockdown TNB-1 cells (left panel: immunostaining of neuritis as described in 'Materials and methods'; right panel: western analysis using indicated antibodies). As a positive control of differentiation, 2.5 μM retinoic acid (RA) was treated 24 h before analysis. AR1, AR2/CR1, CR2: two independent siRNA of ShcA /ShcC; Li: treated with only Lipofectamine 2000; ac1, ac2/cc1, cc2: control siRNA for ShcA /ShcC siRNA, respectively. NC: negative control for universal siRNA (as described in 'Materials and methods').

RNAi (miShcC-1, -2 and -3) were prepared by checking the level of ShcC protein along with clones of LacZ miR RNAi (miLacZ-1 and -2) as controls (Figure 6b). These clones with suppressed level of ShcC showed the same morphological features of neurite formation in tissue culture condition as observed in the cells transfected with ShcC siRNAs (data not shown). The volumes and weights of subcutaneous tumors in nude mice were measured at 6 weeks after injections of the cells and evaluated in at least 4 independent injections per clone. Control LacZ miR RNAi clones (miLacZ-1, miLacZ-2) developed large tumor masses *in vivo* (Figure 6c), whereas remarkable reduction of the size and weight of tumors (or almost disappearance of tumors in some cases) was observed by the stable suppression of ShcC expression. These tumors from ShcC miR RNAi clones showed marked increase in numbers of apoptotic cells compared with control tissues as shown by terminal transferase dUTP nick-end labeling (TUNEL) staining. On the other hand, staining by a proliferation marker, Ki-67 showed no significant difference among each tumor tissue (Figure 6d).

Discussion

It has already been shown that some signal pathways strongly affect tumor progression and treatment resistance (Schwab *et al*., 2003). Other than the Trk family, the PI3K/Akt pathway (Opel *et al*., 2007), Ret (Iwamoto *et al*., 1993; Marshall *et al*., 1997), hepatocyte growth factor/c-Met pathway (Hecht *et al*., 2004) were reported to be closely associated with several diagnostic profiles and biological characteristics of neuroblastoma cells.

This is the first study to show that the expression of ShcC protein, a member of the Shc family docking proteins, is significantly correlated with malignant phenotypes associated with advanced neuroblastoma. Expression of both p52 and p67 isoforms of ShcC,

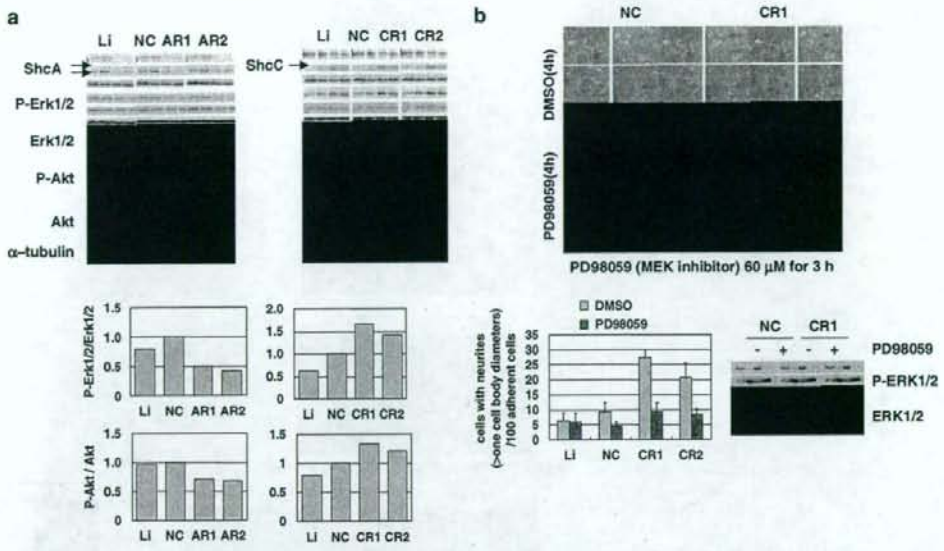

Figure 3 Persistent activation of extracellular signal-related kinase 1/2 (ERK1/2) in ShcC downregulation induces neurite outgrowth in TNB-1 cells. (**a**) Downregulation of ShcC positively affects the ERK1/2 and Akt pathway in TNB-1 cells. Activation of ERK1/2 and Akt in the cells treated with ShcA or ShcC siRNA were examined by western blotting. The levels of activation were quantified comparing to that of cells treated with control siRNA (NC). (**b**) Effect of MEK inhibitor on neurite outgrowth induced by ShcC RNAi in TNB-1 cells. The siRNA-transfected cells indicated were treated with dimethylsulphoxide (DMSO) or PD98059 and incubated for 3 h in the tissue culture condition, then counted for neurite-containing cells.

shows significant correlation with clinical stage and *MYCN* gene amplification whereas the expression of both isoforms of ShcA, p52 and p66, showed little association with those aspects. These results, in the protein level, give further evidence that ShcC is a factor which determines the prognosis of neuroblastoma, which was recently suggested by analysis of the mRNA expression of ShcC (Terui *et al*., 2005).

The biological analysis of TNB-1 cells treated with ShcC-specific siRNAs provided evidence that ShcC protein expressed in the neuroblastoma cells is suppressing the differentiation of neuroblastoma cells. Neurite outgrowth of TNB-1 cells, induced by downregulation of ShcC was dependent on sustained activation of the MEK/ERK pathway. Sustained activation of the ERK pathway triggered by factors such as NGF is required for neuronal differentiation in some neuronal tumor cells such as PC12 cells (Qui and Green, 1992; Yaka *et al*., 1998). The fact that constitutively activated Raf–ERK signaling induced neurite outgrowth in the same cell line (Supplementary Figure C), such as the RTK-related pathway might induce the ERK activation and cellular differentiation in TNB-1 cells, although NGF stimulation failed to induce neurite elongation of TNB-1 cells (data not shown).

Interestingly, elevation in the level of phosphorylated ShcA followed by activation of the ERK pathway by ShcA–Grb2 signals was observed in TNB1 when the ShcC protein expression was suppressed by RNAi. This activation of the ShcA–Grb2–ERK pathway caused by downregulation of ShcC may be due to a competitive effect between ShcC and ShcA for binding to certain RTKs. This possibility is supported by another experiment showing that both EGF-induced phosphorylation of ShcA and complex formation between ShcA and Grb2 in KU-YS cells are suppressed by the expression of ShcC in a dose-dependent manner. It was shown that the expression of the PTB domains of ShcC partially interfered with the binding of endogenous ShcA to activated EGFR in 293 cells (O'Bryan *et al*., 1998). These data are consistent with our current findings described above. It is suspected that some types of differentiation signals mediated by ShcA are blocked by the overexpression of ShcC in some neuroblastoma cells such as TNB-1, and the suppression of ShcC protein by RNAi causes the ShcA-mediated differentiation of these cells.

Elevated level of ShcA phosphorylation and ERK activation induced by ShcC downregulation was more significant under the stimulation of collagen I than without any ECM stimulation. In addition, in suspending condition we could not detect any activation of ShcA nor ERK signal after ShcC downregulation (Supplementary Figure E). These results indicate that the difference between ShcA and ShcC might be in interaction with matrix-adhesion signals. ShcA is considered to be implicated in the adherent related pathway, phosphorylated by forming a complex with

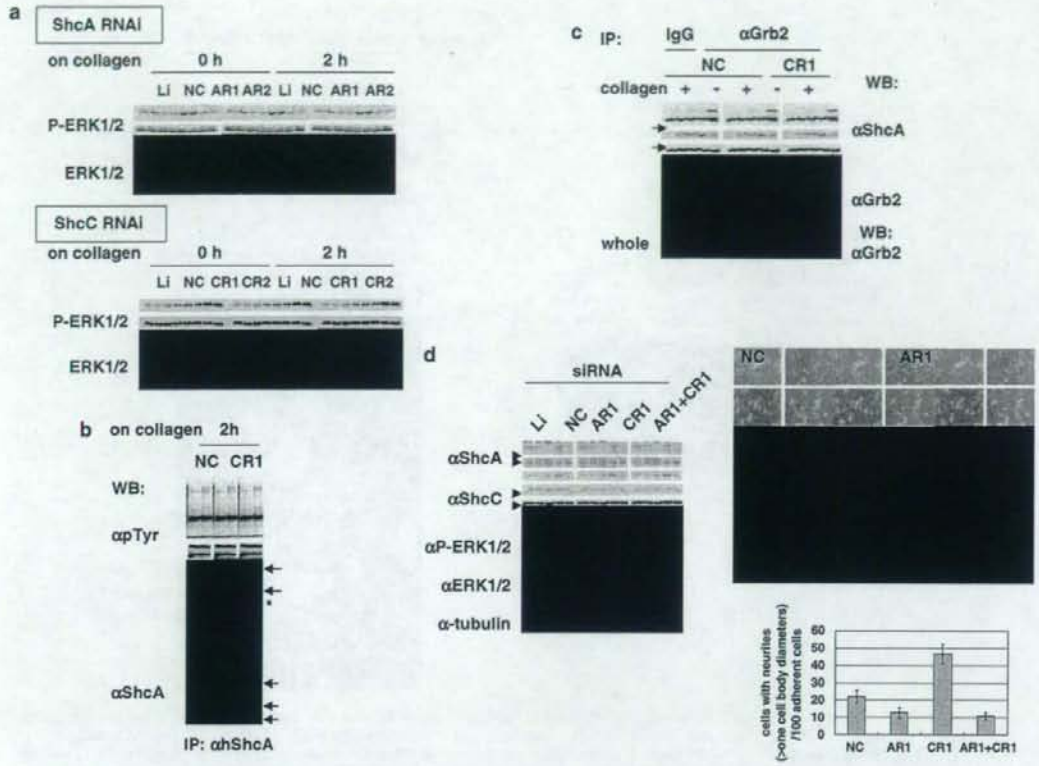

Figure 4 Elevation of extracellular signal-regulated kinase ()-activated level in ShcC-knockdown cells is increased by collagen stimulation by ShcA–Grb2 signaling. (**a**) Elevation of the ERK1/2-activated level due to ShcC downregulation is further increased 2 h after collagen stimulation. siRNAs of ShcA/ShcC-transfected TNB-1 cells (AR1, AR2/CR1, CR2, respectively) were incubated in the tissue culture condition for 70 h and stimulated by collagen type I. Duplicated cells were harvested 0 and 2 h after collagen stimulation (as described in 'Materials and methods'). (**b**) After collagen stimulation ShcA was phosphorylated more strongly in ShcC-knockdown cells than the control cells. Asterisks show heavy chains of immunoglobulin. (**c**) ShcA–Grb2 complex formation (upper panel) were increased by downregulation of ShcC. (**d**) The ShcA-knockdown effect on the neurite outgrowth in cells transfected with ShcC siRNA was evaluated by the same method performed in Figure 2Ba. The number of neurites observed in the cells transfected with both ShcA and ShcC siRNA was obviously decreased compared to cells transfected with only ShcC siRNA.

Fyn (Wary *et al*., 1998) through its proline-rich region that is not conserved in ShcC.

In tissue culture and in transgenic mice, signaling through Fyn has been closely associated with neurite extension and cell adhesion (Brouns *et al*., 2000, 2001). Berwanger *et al*. (2002) referred to the inverse correlation between the expression of Fyn and progression of neuroblastoma from 94 primary neuroblastoma specimens, showing that expressed Fyn-induced differentiation and growth arrest of neuroblastoma cell lines. Another report indicated that active Fyn kinase induces a lasting activation of the MAPK pathway through inhibition of MAPK phosphatase 1 (Wellbrock *et al*., 2002). We confirmed that neurite outgrowth of ShcC-knockdown TNB-1 cells was suppressed by Src family inhibitor, PP2 (Supplementary Figure H). These data suggest the possibility that Integrin–Fyn–ShcA signals could be closely associated with the differentiation of TNB-1 cells induced by ShcC downregulation along with the signals of RTK–ShcA/ShcC.

Noticeably, the interference of the ShcA-mediated signaling by ShcC protein is independent of tyrosine phosphorylation of ShcC. The function of the nonphosphorylated domain of ShcC such as SH2 might be also highlighted. As for the difference in the downstream signaling between ShcC and ShcA, little is known so far. Regarding to this point, Nakamura *et al*. (2002) indicated that inhibition of NGF-induced ERK activation by the expression of ShcC was due to the different Grb2-binding capacity between ShcA and ShcC in response to NGF. It was previously reported that ShcA preferentially binds to TrkA (Yamada *et al*., 2002), which is the key receptor against NGF due to neurite outgrowth with the sustained ERK phosphorylation,

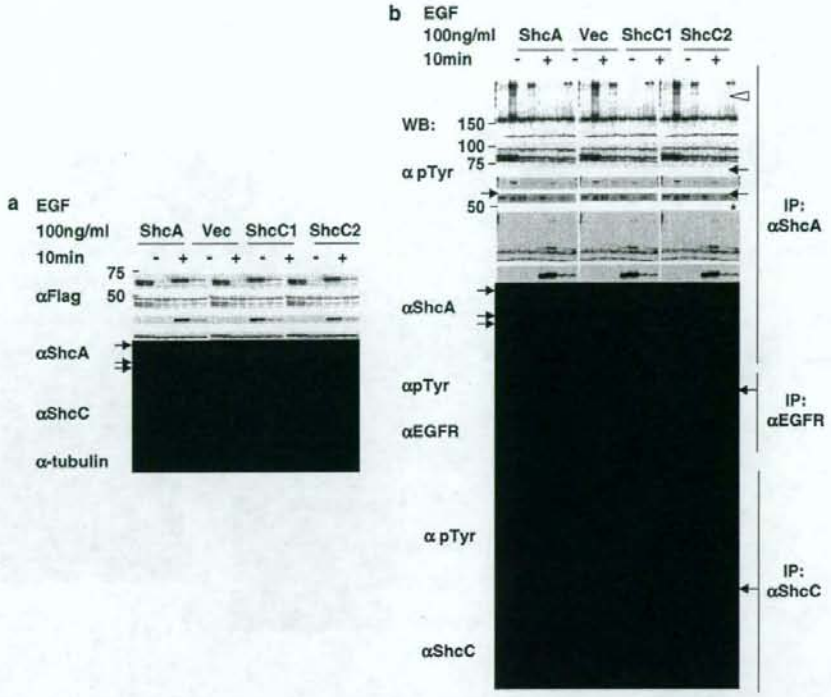

Figure 5 High expression of ShcC suppresses the phosphorylation of ShcA in KU-YS cells stimulated by epidermal growth factor (EGF). We generated stable clones of KU-YS cells expressing Flag-tagged ShcA and diverse levels of p52ShcC (ShcC1 and ShcC2) other than clones transfected with the control vector. (**a**) Each expression level was detected by western analysis. (**b**) Levels of expression and tyrosine phosphorylation of EGFR (middle panel), ShcA (upper panel) and ShcC (lower panel) were analysed by immunoprecipitation and immunoblotting using the antibodies indicated in figure in the KU-YS clone cells stimulated by EGF (as described in 'Materials and methods'). Asterisks show heavy chains of immunoglobulin.

whereas ShcC associated with TrkB rather than TrkA (O'Bryan *et al*., 1998; Liu and Meakin, 2002). In neuroblastoma, the function of signal pathways downstream of these two neurotrophin receptors might be quite different (Nakagawara *et al*., 1993), also suggesting the distinct function of downstream signal mediated by ShcC.

The effect of ShcC knockdown in *in vivo* tumorigenicity was quite remarkable comparing the effect in growth rate in tissue culture condition. We found that anchorage-independent growth in cells was also dramatically decreased by knockdown of ShcC as shown by soft agar assay (Figure 6a). Furthermore, the proportion of apoptotic cells in the nude mouse tumors generated from neuroblastoma cells *in vivo* was remarkably increased by the knockdown of ShcC. In recent study, Magrassi *et al*. (2005) showed that ShcC positively effects on cell survival by PI3K–AKT pathway in glioma cells using dominant negative form of ShcC. Theses data indicate that ShcC has additional function in the protection from some types of apoptosis in addition to the induction of differentiation of cells.

It was indicated that ShcC might have a potent function for tumor progression in neuroblastoma by suppressing the differentiation and by promoting the anchorage-independent growth in the majority of neuroblastoma cells which has high expression of ShcC protein. From these points of view, we suggest that ShcC is a potent tool for predicting the phenotype of neuroblastoma and is also a good candidate for therapeutic targets of advanced neuroblastoma.

Materials and methods

Cell culture and tissue samples

DLD-1 cells and all cell lines of neuroblastomas in this study were prepared as described in the previous report (Miyake *et al*., 2002). These cells were cultured in an RPMI 1640 medium with 10% fetal calf serum (FCS) (Sigma, St Louis, MO, USA) at 37 °C in an atmosphere containing 5% CO_2.

Anonymous 46 frozen neuroblastoma tissues were used in this study. The samples were divided into three subsets using Brodeur's classification; type I (stage 1, 2 or 4S; a single copy of *MYCN*), type II (stage 3 or 4; a single copy of *MYCN*) and type III (all stages; amplification of *MYCN*) (Brodeur and Nakagawara, 1992; Ohira *et al*., 2003). A total of 15 samples belonged to type I, 18 samples to type II and 13 samples to type III. Staging classification was according to the